2019-16

Working paper. Economics

ISSN 2340-5031

MARKOV-SWITCHING SCORE-DRIVEN MULTIVARIATE MODELS: OUTLIER-ROBUST MEASUREMENT OF THE RELATIONSHIPS BETWEEN WORLD CRUDE OIL PRODUCTION AND US INDUSTRIAL PRODUCTION

Szabolcs Blazsek[a,*], Alvaro Escribano[b], and Adrian Licht[a]

[a]*School of Business, Universidad Francisco Marroquín , Guatemala City, Guatemala*
[b]*Department of Economics, Universidad Carlos III de Madrid, Spain*

uc3m | Universidad Carlos III de Madrid

Serie disponible en http://hdl.handle.net/10016/11

Web: http://economia.uc3m.es/

Correo electrónico: departamento.economia@eco.uc3m.es

Markov-switching score-driven multivariate models: outlier-robust measurement of the relationships between world crude oil production and US industrial production

Szabolcs Blazsek [a,*], Alvaro Escribano [b], and Adrian Licht [a]

[a] *School of Business, Universidad Francisco Marroquín, Guatemala City, Guatemala*

[b] *Department of Economics, Universidad Carlos III de Madrid, Getafe (Madrid), Spain*

Abstract: In this paper, new Seasonal-QVAR (quasi-vector autoregressive) and Markov switching (MS) Seasonal-QVAR (MS-Seasonal-QVAR) models are introduced. Seasonal-QVAR is an outlier-robust score-driven state space model, which is an alternative to classical multivariate Gaussian models (e.g. basic structural model; Seasonal-VARMA). Conditions of the maximum likelihood estimator and impulse response functions are shown. Dynamic relationships between world crude oil production and US industrial production are studied for the period of 1973 to 2019. Statistical performances of alternative models are analyzed. MS-Seasonal-QVAR identifies structural changes and extreme observations in the dataset. MS-Seasonal-QVAR is superior to Seasonal-QVAR and, and both are superior to Gaussian alternatives.

Keywords: World crude oil production; United States industrial production; Dynamic conditional score models; Score-driven multivariate stochastic location and stochastic seasonality models; Markov regime-switching models

JEL classification codes: C32; C51; C52

*Corresponding author. School of Business, Universidad Francisco Marroquín, Calle Manuel F. Ayau, Guatemala City 01010, Guatemala. *E-mail address:* sblazsek@ufm.edu

1. Introduction

In this paper, new dynamic time series models are developed for the world crude oil supply and US industrial production relation. The new models are robust to extreme observations and structural changes, and their proposal is motivated by the following recent economic events and technological developments: First, the recently increased crude oil production capabilities of the US may indirectly influence US industrial production. In April 2019, the US crude oil production surpassed the 12 million barrels per day level for the first time in history (International Energy Agency), which is at least partly due to the improved fracking technologies (US Energy Information Administration). In relation to this, the International Energy Agency predicts that the US will remain the top crude oil producing country of the world for the next five years. Second, after the renegotiation of the North American Free Trade Agreement (NAFTA), the recently signed US–Mexico–Canada Agreement (USMCA) may imply changes in the levels of industrial production and crude oil production of the US, Mexico and Canada, because these countries are the largest commercial partners among each other and are also among the largest crude oil producers in the world (International Energy Agency). Third, several recent works study the implications of the unconventional monetary policy after the 2008 US financial crisis (e.g. Cukierman, 2013; Chen et al., 2016; Francis et al., 2019). Our analysis of the world crude oil production and US industrial production relation contributes to that literature, due to the following reasons. Central banks closely monitor the changes in industrial production, because effective industrial production forecasts help in the determination of inflation targets and interest rates (e.g. Romer et al., 1990). According to Friedman (1977), increases in inflation volatility should reduce the level of industrial production. Crude oil price volatility that is induced by oil supply shocks may result in inflation volatility and influence the US real economic activity. Bernanke et al. (1997) conclude that: (i) monetary policy response is the dominant source of the real effects of an oil price shock, and (ii) the initial oil price shock does show a substantial inflationary impact in the short run. Thus, the practical use of the new models may be considered by policymakers in the Federal Reserve System.

Kilian (2008a) shows that an energy price increase that is driven by adverse global oil supply shocks may have more significant consequences on the United States (US) real output than oil demand shocks. Motivated by this, the present paper focuses on world crude oil production and US industrial production: Crude oil supply shocks are measured by using unexpected changes in world crude oil production (Baumeister and Peersman, 2013; Baumeister and Hamilton, 2017; Kilian and Lütkepohl,

2017). Moreover, the use of the US industrial production is motivated by the work of Bernanke et al. (1997), which considers that variable as a possible measure of economic output. Future extensions of the present work may consider additional macroeconomic variables from the literature (Baumeister and Peersman, 2013; Baumeister and Hamilton, 2017).

The econometric methods that are used in the work of Bernanke et al. (1997) have been criticized, with respect to the relatively short lag-order selection, for example, in the work of Hamilton and Herrera (2004). We believe that, in addition to the correct lag-order selection in the VAR (vector autoregressive) models, a further important issue is the effective treatment of extreme shocks and structural changes that influence crude oil production and US industrial production (e.g. Balke and Fomby, 1994; Pestana Barros et al., 2011). The main contribution of the present paper is to suggest the practical use of a new outlier-robust multivariate dynamic econometric model for policy makers, in order to analyze the response of the output of the US economy to global crude oil supply shocks. The use of the Seasonal-QVAR (quasi-VAR) model, which includes score-driven multivariate stochastic local level and stochastic seasonality components, is suggested. Seasonal-QVAR is a dynamic conditional score (DCS) model (Creal et al., 2011, 2013; Harvey, 2013), in which the conditional score of the log-likelihood (LL) (hereinafter, score function) updates the dependent variables and the noise term has a multivariate t-distribution. An important property of Seasonal-QVAR, as opposed to multivariate time series models with Gaussian error terms, is that the QVAR filter is robust to extreme values. In this paper, the results of Harvey (2013) and Blazsek et al. (2017) are extended to Seasonal-QVAR, by deriving the (i) nonlinear infinite vector moving average VMA(∞) representation of the local level component, (ii) formulas for the impulse response functions (IRFs), and (iii) conditions of consistency and asymptotic normality of the maximum likelihood (ML) estimator. In order to perform robustness analysis about the dynamics of the world crude oil production and US industrial production relationship, Seasonal-QVAR is extended to Markov regime-switching Seasonal-QVAR (MS-Seasonal-QVAR) (e.g. Hamilton, 1989; Kim and Nelson, 1999). MS-Seasonal-QVAR identifies structural changes and outliers for world crude oil production and US industrial production.

We use monthly time series data on world crude oil production growth and US industrial production growth for the period of March 1973 to April 2019. Thus, the present paper extends the sample period of previous studies on crude oil and industrial production (e.g. Nordhaus et al., 1980; Kilian, 2008b; Peersman and Van Robays, 2009; Baumeister and Peersman, 2013). Both variables have significant

seasonality components (Ye et al., 2006 and Raunglerdpanyagul, 1985, respectively), and the dataset includes several extreme observations (e.g. related to the 1973 and 1979 oil crises).

Seasonal-QVAR disentangles the local level and the stochastic seasonality components, as seasonality effects do not appear in the IRF estimates of Seasonal-QVAR. The statistical performance of Seasonal-QVAR is superior to the statistical performances of the Gaussian multivariate unobserved components model (UCM) with local level and stochastic seasonality (hereinafter, basic structural model) (Harvey, 1989) and Gaussian Seasonal-VARMA (e.g. Lütkepohl, 2005). Furthermore, MS-Seasonal-QVAR indicates a structural change in the world crude oil production growth and US industrial production growth variables in June 1992 and also highlights several outliers within the sample period. For MS-Seasonal-QVAR, conditions of consistency and asymptotic normality of the ML estimator are satisfied. MS-Seasonal-QVAR is superior to Seasonal-QVAR, and both models are superior to the Gaussian multivariate alternatives. The best-performing MS-Seasonal-QVAR specification with two dependent variables provides IRF estimates for the world crude oil production and US industrial production relation, that are similar to the IRFs reported in the works of Baumeister and Peersman (2013) and Baumeister and Hamilton (2017). The new score-driven multivariate models of this paper provide better measurements of dynamic interaction effects than classical multivariate models for crude oil production and industrial production. Therefore, the practical use of the new models may be considered by policymakers, for example, in the Federal Reserve System.

The remainder of this paper is organized as follows: Section 2 reviews the relevant literature. Section 3 presents Seasonal-QVAR. Section 4 presents the Gaussian multivariate alternatives. Section 5 describes the dataset. Section 6 summarizes the results for Seasonal-QVAR and the Gaussian multivariate alternatives. Section 7 presents MS-Seasonal-QVAR for robustness analysis. Section 8 concludes.

2. Literature review

2.1. Crude oil prices and read economic activity

The relationships between crude oil price shocks and real economic activity are extensively studied in the literature (see e.g. Bernanke et al., 1997; Barsky and Kilian, 2002; Kilian, 2008a, 2009, 2010; Elder and Serletis, 2010; Blanchard and Riggi, 2013). The works of Kilian (2009, 2010) note that crude oil prices are driven by distinct shocks which are: (i) shocks from global demand for industrial commodities, (ii) crude oil market-specific demand shocks, and (iii) crude oil supply shocks. Each of those shocks has different dynamic effects on the real price of crude oil, which may shed light on the

fact that regressions of macroeconomic aggregates on crude oil prices tend to be unstable (Guo and Klisen, 2005; Kilian, 2009, 2010; Alquist et al., 2011). Crude oil supply shocks have been studied in several works in the body of literature (e.g. Nordhaus et al., 1980; Hamilton 2003; Kilian, 2008a, 2008b; Peersman and Van Robays, 2009; Baumeister and Peersman, 2013; Baumeister and Kilian, 2014; Baumeister and Hamilton, 2017; Kilian and Lütkepohl, 2017). Kilian (2008a) shows that an energy price increase that is driven by a strong global demand for crude oil may have less adverse consequences for US real output than the same energy price increase that is driven by adverse global oil supply shocks (see also Kilian and Lewis, 2011). The analysis of the world crude oil production and US industrial production relations of the present paper is in close relation to the works of Baumeister and Peersman (2013), Baumeister and Hamilton (2017), and Kilian and Lütkepohl (2017, Chapter 12.13).

2.2. DCS models

DCS models are observation-driven time series models (Cox, 1981). Due to the score-driven updating mechanism of DCS models, the information gain in the filters is optimal according to the Kullback–Leibler divergence measure (Blasques et al., 2015). An example of DCS models is the Beta-t-GARCH (generalized autoregressive conditional heteroskedasticity) model (Harvey and Chakravarty, 2008), which is an extension of the GARCH model (Engle, 1982; Bollerslev, 1986). Another example is the QAR model (Harvey, 2013), which is an extension of the ARMA model (Box and Jenkins, 1970). With respect to recent DCS models, we refer to the following works: Blazsek and Escribano (2016) suggest a DCS count panel data model, which is an alternative to the dynamic count panel data models of Blundell et al. (2002), Wooldridge (2005) and Blazsek and Escribano (2010, 2016). Ayala et al. (2019) suggest DCS-EGARCH (exponential GARCH) models with score-driven shape parameters, which are extensions of the DCS-EGARCH models with constant shape parameters (e.g. Harvey, 2013). Blazsek et al. (2019) present QVARMA models for combinations of $I(0)$ and co-integrated $I(1)$ variables (e.g. Hamilton, 1994), in order to study the dynamic relations between the effective federal funds rate and the US inflation rate.

Seasonal-QVAR is an alternative to the basic structural model (Harvey, 1989), which is a widely-used model for macroeconomic and financial time series variables. Seasonal-QVAR is an extension of QVAR (Harvey, 2013; Blazsek et al., 2017), that is also named as the dynamic conditional score model for the multivariate t-distribution (Harvey, 2013). Motivated by successful applications of DCS seasonality models to univariate variables (Harvey, 2013; Harvey and Luati, 2014; Caivano et al., 2016;

Blazsek and Hernández, 2018; Ayala and Blazsek, 2018, 2019), in the present paper QVAR is extended by adding a multivariate score-driven seasonality component. This paper is also related to the body of literature on VAR and VARMA models (e.g. Lütkepohl, 2005), because Seasonal-QVAR is a nonlinear extension of Gaussian Seasonal-VARMA.

3. Score-driven multivariate models

3.1. Seasonal-QVAR

For the dependent variables y_t $(K \times 1)$ with $t = 1, \ldots, T$, Seasonal-QVAR is $y_t = c + \mu_t + s_t + v_t$, where c $(K \times 1)$ is the vector of constant parameters, μ_t $(K \times 1)$ is the local level component, s_t $(K \times 1)$ is the seasonality component, and v_t $(K \times 1)$ is the reduced-form error term. Components μ_t and s_t are observable, conditional on $(y_1, \ldots, y_{t-1})$. The reduced-form error term v_t is specified as multivariate i.i.d. $v_t \sim t_K(0, \Sigma_v, \nu)$, where $\Sigma_v = \Omega_v^{-1}(\Omega_v^{-1})'$ is positive definite and $\nu > 2$ is the degrees of freedom parameter (hence, the covariance matrix of v_t is well-defined). As a consequence, $E(v_t) = 0$ and $\text{Var}(v_t) = \Sigma_v \times \nu/(\nu-2)$. The multivariate i.i.d. structural-form error term is $\epsilon_t = [\nu/(\nu-2)]^{-1/2}\Omega_v \times v_t$, for which $E(\epsilon_t) = 0$ and $\text{Var}(\epsilon_t) = I_K$. The log of the conditional density of y_t is

$$\ln f(y_t|y_1, \ldots, y_{t-1}; \Theta) = \ln \Gamma\left(\frac{\nu + K}{2}\right) - \ln \Gamma\left(\frac{\nu}{2}\right) - \frac{K}{2}\ln(\pi\nu) \tag{1}$$

$$-\frac{1}{2}\ln|\Sigma_v| - \frac{\nu + K}{2}\ln\left(1 + \frac{v_t'\Sigma_v^{-1}v_t}{\nu}\right)$$

where Θ denotes the vector of parameters. The score function with respect to μ_t is

$$\frac{\partial \ln f(y_t|y_1, \ldots, y_{t-1}; \Theta)}{\partial \mu_t} = \frac{\nu + K}{\nu}\Sigma_v^{-1} \times \left(1 + \frac{v_t'\Sigma_v^{-1}v_t}{\nu}\right)^{-1} v_t = \frac{\nu + K}{\nu}\Sigma_v^{-1} \times u_t \tag{2}$$

where u_t $(K \times 1)$ is the scaled score function vector, which is multivariate i.i.d. with zero mean and well-defined covariance matrix (Harvey, 2013). In the definition of the score function, v_t is multiplied by the term $[1 + (v_t'\Sigma_v^{-1}v_t)/\nu]^{-1} = \nu/(\nu + v_t'\Sigma_v^{-1}v_t) \in (0, 1)$. As a consequence, the score function is always bounded by the reduced-form error term: $|u_t| < |v_t|$.

The local level component is $\mu_t = \Phi\mu_{t-1} + \Psi u_{t-1}$, where Φ $(K \times K)$ and Ψ $(K \times K)$ are time-constant parameter matrices, and μ_t is updated by the first lag of the scaled score function u_{t-1}. Let C_1 denote the maximum modulus of eigenvalues of Φ. If $C_1 < 1$, then $E(\mu_t) = 0$. Local level μ_t is initialized by using the unconditional mean $\mu_1 = E(\mu_t) = 0_{K\times 1}$. The QVAR(1) specification of this

paper can be extended to higher order QVAR(p) specifications in future works in a straightforward way. The consideration of first-order dynamic models is motivated by the fact that a bottom-up model specification strategy is used in the present paper (Krolzig, 1997).

The seasonality component s_t is specified as follows: Each element of the seasonality component $s_t = (s_{1,t}, \ldots, s_{K,t})'$ is formulated according to $s_{k,t} = D_t' \rho_{k,t}$ for each $k = 1, \ldots, K$, where $D_t = (D_{1,t}, \ldots, D_{S,t})'$ is a vector of seasonal dummy variables and $\rho_{k,t} = (\rho_{k,1,t}, \ldots, \rho_{k,S,t})'$ is a vector of dynamic seasonality parameters (S denotes the known period of the seasonality). Variable $\rho_{k,t}$ is updated according to the $I(1)$ equation $\rho_{k,t} = \rho_{k,t-1} + \gamma_{k,t} u_{k,t-1}$, where $\gamma_{k,t} = (\gamma_{k,1,t}, \ldots, \gamma_{k,S,t})'$ is a dynamic scaling parameter and $u_{k,t-1}$ is the k-th element of u_{t-1}. From Equation (1), it follows that $\partial \ln f(y_t|y_1, \ldots, y_{t-1})/\partial \mu_t = \partial \ln f(y_t|y_1, \ldots, y_{t-1})/\partial s_t$, hence the same updating term u_{t-1} is used for μ_t and s_t, which motivates the joint estimation of μ_t and s_t. Furthermore, each element of $\gamma_{k,t}$ is given by $\gamma_{k,j,t} = \gamma_{k,j}$ for $D_{j,t} = 1$ and $\gamma_{k,j,t} = -\gamma_{k,j}/(S-1)$ for $D_{j,t} = 0$, where $\gamma_{k,j}$ with $j = 1, \ldots, S$ are seasonality parameters to be estimated. This parameterization ensures that $\sum_{j=1}^{S} \gamma_{k,j,t} = 0$. In relation to this, it is shown in the Appendix A that $s_{k,t}$ is centered at zero. Variable $s_{k,t}$ is the output of a high-pass filter that compensates the unit root in $\rho_{k,t}$ (Baxter and King, 1999), which is necessary since $y_{k,t}$ is $I(0)$. Variable $\rho_{k,t}$ is initialized by using a first-step nonlinear least squares (NLS) procedure, in which $y_{k,t}$ is regressed on the seasonal dummy variables (Harvey, 2013).

3.2. IRFs

In Seasonal-QVAR, the local level component μ_t measures all dynamic interaction effects among y_t. The structural-form nonlinear VMA(∞) representation of μ_t is:

$$\mu_t = \sum_{j=0}^{\infty} \Phi^j \Psi [(\nu-2)\nu]^{1/2} \Omega_v^{-1} \frac{\epsilon_{t-1-j}}{\nu - 2 + \epsilon_{t-1-j}' \epsilon_{t-1-j}} \tag{3}$$

If $C_1 < 1$, then the series in the previous equation is convergent. Then, $\text{IRF}_{j,t} = \partial \mu_{t+j}/\partial \epsilon_{t-1} = \Phi^j \Psi [(\nu-2)\nu]^{1/2} \Omega_v^{-1} Q_{t-1-j}$ for $j = 0, 1, \ldots, \infty$, where

$$Q_t = \frac{\partial \frac{\epsilon_t}{\nu - 2 + \epsilon_t' \epsilon_t}}{\partial \epsilon_t} = \begin{bmatrix} q_{1,1,t} & \cdots & q_{1,K,t} \\ \cdots & \cdots & \cdots \\ q_{K,1,t} & \cdots & q_{K,K,t} \end{bmatrix} = \tag{4}$$

$$= \begin{bmatrix} \frac{\nu-2+\epsilon_t'\epsilon_t-2\epsilon_{1,t}^2}{(\nu-2+\epsilon_t'\epsilon_t)^2} & \frac{-2\epsilon_{1,t}\epsilon_{2,t}}{(\nu-2+\epsilon_t'\epsilon_t)^2} & \cdots & \frac{-2\epsilon_{1,t}\epsilon_{K,t}}{(\nu-2+\epsilon_t'\epsilon_t)^2} \\ \frac{-2\epsilon_{2,t}\epsilon_{1,t}}{(\nu-2+\epsilon_t'\epsilon_t)^2} & \frac{\nu-2+\epsilon_t'\epsilon_t-2\epsilon_{2,t}^2}{(\nu-2+\epsilon_t'\epsilon_t)^2} & \cdots & \cdots \\ \cdots & \cdots & \cdots & \cdots \\ \frac{-2\epsilon_{K,t}\epsilon_{1,t}}{(\nu-2+\epsilon_t'\epsilon_t)^2} & \cdots & \cdots & \frac{\nu-2+\epsilon_t'\epsilon_t-2\epsilon_{K,t}^2}{(\nu-2+\epsilon_t'\epsilon_t)^2} \end{bmatrix}$$

IRF is time-varying for QVAR, due to the presence of Q_{t-1-j} in the IRF formula. In the empirical application of this paper, the following unconditional mean of $\text{IRF}_{j,t}$ is used: $\text{IRF}_j = E(\text{IRF}_{j,t}) = \Phi^j \Psi[(\nu-2)\nu]^{1/2}\Omega_v^{-1}E(Q_{t-1-j})$ for $j = 0, 1, 2, \ldots, \infty$. The expected value $E(Q_{t-1-j})$ is estimated by using the sample average of Q_t for $t = 1, \ldots, T$. The use of this estimator is supported by using the augmented Dickey–Fuller (ADF, Dickey and Fuller 1979) test with constant for each element of Q_t. An alternative to the use of the time-invariant $E(\text{IRF}_{j,t})$ is the period-by-period estimation and analysis of $\text{IRF}_{j,t}$. In those applications, $\text{IRF}_{j,t}$ can be averaged for different subperiods of the dataset (for example, for pre- and post-oil crisis periods) and those averages can be compared. The IRF confidence interval is estimated by using 10,000 Monte Carlo simulations.

3.3. Statistical inference of Seasonal-QVAR

It is popular among practitioners to apply the following two-step estimation procedure to macroeconomic variables that involve seasonality components: Deseasonalize the macroeconomic time series in a first step, and undertake an IRF analysis in a second step for the deseasonalized time series. That approach assumes that the seasonal and non-seasonal shocks are uncorrelated, which may fail in practice. The two-step estimation procedure is not effective for Seasonal-QVAR, because both the local level component and the stochastic seasonality component are updated by the same score function term. In Seasonal-QVAR, the seasonal and non-seasonal shocks are correlated, motivating the joint estimation of multivariate local level and stochastic seasonality. In the present paper an alternative to the UCM specification of Hindrayanto et al. (2018) is suggested, in which local level and stochastic seasonality with correlated seasonal and non-seasonal shocks are jointly estimated.

Seasonal-QVAR is estimated by using the maximum likelihood (ML) method:

$$\hat{\Theta}_{\text{ML}} = \arg\max_{\Theta} \text{LL}(y_1, \ldots, y_T; \Theta) = \arg\max_{\Theta} \sum_{t=1}^{T} \ln f(y_t|y_1, \ldots, y_{t-1}; \Theta), \tag{5}$$

where $\ln f(y_t|y_1, \ldots, y_{t-1}; \Theta)$ is defined in Equation (1). Estimations are performed by using alternative

start values of parameters, in order to find a global maximum. In the numerical maximization of the LL function, the convergence tolerance for gradient is 10^{-5} for all the parameters. The inverse information matrix is used for the estimation of the standard errors of $\hat{\Theta}_{\mathrm{ML}}$ (Harvey, 2013). The standard errors of transformed parameters are computed by using the delta method.

The following conditions allow the use of the ML estimator, because they ensure the covariance stationarity of μ_t and the consistent estimation of the corresponding elements of the information matrix (Harvey, 2013). For the parameters in s_t, the conditions of ML are satisfied because the parameters of $\rho_{k,t-1}$ are set to the identity matrix (i.e. multivariate random walk) in $\rho_{k,t} = \rho_{k,t-1} + \gamma_{k,t} u_{k,t-1}$. If the unit root is imposed rather than estimated in DCS models, then the standard asymptotics of ML apply (Harvey 2013). First, Condition 1 is $C_1 < 1$, which is equivalent to μ_t being covariance stationary. Second, Condition 2 holds if $E[u_{j,t}^{2-i}(\partial u_{k,t}/\partial \mu_{l,t})^i] < \infty$, where $i = 0, 1, 2$ and $j, k, l = 1, \ldots, K$. For those expectations the sample average estimator is used, and the use of that estimator is supported by using the ADF test with constant. Third, for Condition 3 the representative element $\Psi_{i,j}$ is considered from the matrix Ψ. The derivative of the local level μ_t with respect to $\Psi_{i,j}$ is:

$$\frac{\partial \mu_t}{\partial \Psi_{i,j}} = \Phi \frac{\partial \mu_{t-1}}{\partial \Psi_{i,j}} + \Psi \frac{\partial u_{t-1}}{\partial \Psi_{i,j}} + W_{i,j} u_{t-1} \tag{6}$$

for all $t = 1, \ldots, T$, where the element (i, j) of the matrix $W_{i,j}$ $(K \times K)$ is one and the rest of the elements of $W_{i,j}$ are zero. By using the chain rule, Equation (6) is written as

$$\frac{\partial \mu_t}{\partial \Psi_{i,j}} = \left(\Phi + \Psi \frac{\partial u_{t-1}}{\partial \mu'_{t-1}} \right) \frac{\partial \mu_{t-1}}{\partial \Psi_{i,j}} + W_{i,j} u_{t-1} = X_t \frac{\partial \mu_{t-1}}{\partial \Psi_{i,j}} + W_{i,j} u_{t-1}. \tag{7}$$

Condition 3 is that all eigenvalues of $E(X_t)$ are within the unit circle, where the finiteness of all elements of $E(X_t)$ follows from Condition 2. The maximum modulus of eigenvalues of $E(X_t)$ is denoted by using C_3. Each element of $E(X_t)$ is estimated by using the sample average, which is supported by the ADF test. For the computation of X_t, the derivative $\partial u_{t-1}/\partial \mu'_{t-1}$ $(K \times K)$ is available by using standard matrix calculus. Fourth, for Condition 4, the information matrix depends on:

$$\frac{\partial \mu_t}{\partial \Psi_{i,j}} \frac{\partial \mu'_t}{\partial \Psi_{k,l}} = X_t \frac{\partial \mu_{t-1}}{\partial \Psi_{i,j}} \frac{\partial \mu'_{t-1}}{\partial \Psi_{k,l}} X'_t + X_t \frac{\partial \mu_{t-1}}{\partial \Psi_{i,j}} W'_{i,j} u_{t-1} + u'_{t-1} W_{k,l} \frac{\partial \mu'_{t-1}}{\partial \Psi_{k,l}} X'_t + W_{i,j} u_{t-1} u'_{t-1} W'_{k,l} \tag{8}$$

that can also be written as:

$$\text{vec}\left(\frac{\partial \mu_t}{\partial \Psi_{i,j}}\frac{\partial \mu_t'}{\partial \Psi_{k,l}}\right) = (X_t \otimes X_t)\text{vec}\left(\frac{\partial \mu_{t-1}}{\partial \Psi_{i,j}}\frac{\partial \mu_{t-1}'}{\partial \Psi_{k,l}}\right) \tag{9}$$

$$+\text{vec}\left(X_t\frac{\partial \mu_{t-1}}{\partial \Psi_{i,j}}W_{i,j}'u_{t-1}\right) + \text{vec}\left(u_{t-1}'W_{k,l}\frac{\partial \mu_{t-1}'}{\partial \Psi_{k,l}}X_t'\right) + \text{vec}\left(W_{i,j}u_{t-1}u_{t-1}'W_{k,l}'\right),$$

where $\otimes$ is the Kronecker product and vec(x) indicates that the columns of the matrix are being stacked one upon the other. Condition 4 is that all eigenvalues of $E(X_t \otimes X_t)$ are within the unit circle, where the finiteness of all elements of $E(X_t \otimes X_t)$ follows from Condition 2. The maximum modulus of eigenvalues of $E(X_t \otimes X_t)$ is denoted by using C_4. Each element of $E(X_t \otimes X_t)$ is estimated by using the sample average estimator, which is supported by the ADF test with constant.

4. Classical alternatives

4.1. Limiting special case: Gaussian Seasonal-VARMA

Seasonal-QVAR can be related to the Gaussian Seasonal-VARMA and Gaussian Seasonal-VAR models (e.g. Lütkepohl 2005). If $\nu \to \infty$, then $v_t \to_d N_K(0, \Sigma_v)$ and $u_t \to_p v_t$; Equation (2). From equations $y_t = c + \mu_t + s_t + v_t$ and $\mu_t = \Phi\mu_{t-1} + \Psi u_{t-1}$, the following Gaussian Seasonal-QVAR model is obtained, as a limiting special case: $y_t = (I_K - \Phi)c + \Phi y_{t-1} + (I_K - \Phi L)s_t + (\Psi - \Phi)v_{t-1} + v_t$. Thus, Seasonal-QVAR becomes Gaussian Seasonal-VARMA, in which the error term v_t has a multivariate i.i.d. Gaussian distribution and both local level μ_t and stochastic seasonality s_t are updated by v_{t-1}. Gaussian Seasonal-VARMA is a special case of Seasonal-QVAR for large ν. Furthermore, Gaussian Seasonal-VAR is another special case of Seasonal-QVAR for large ν and $\Psi = \Phi$. In this paper, the more general Gaussian Seasonal-VARMA alternative is estimated. For Seasonal-VARMA, the local level μ_t measures all dynamic interaction effects among y_t. The VMA(∞) representation of the local level is $\mu_t = \sum_{j=0}^{\infty} \Phi^j \Psi \Omega_v^{-1} \epsilon_{t-1-j}$, which is obtained by using the decomposition $\Sigma_v = \Omega_v^{-1}(\Omega_v^{-1})'$. Let C_1 denote the maximum modulus of eigenvalues of Φ. If $C_1 < 1$, then the series in the VMA(∞) representation is finite. For Seasonal-VARMA, $\text{IRF}_{j,t} = \partial \mu_{t+j}/\partial \epsilon_{t-1} = \Phi^j \Psi \Omega_v^{-1}$ for $j = 0, 1, \ldots, \infty$. Seasonal-VARMA is estimated by using the ML method. Even if the $v_t \sim N_K(0, \Sigma_v)$ assumption does not hold, the ML estimator still provides consistent and asymptotically normal parameter estimates for Seasonal-VARMA, according to the quasi-ML (QML) results of Gouriéroux et al. (1984).

4.2. Basic structural model

The basic structural model is $y_t = c + \mu_t + s_t + v_t$, where c $(K \times 1)$ includes constant parameters, μ_t $(K \times 1)$ is the local level, s_t $(K \times 1)$ is the stochastic seasonality, and $v_t \sim N_K(0_{K\times 1}, \Sigma_v) = N_K[0_{K\times 1}, \Omega_v^{-1}(\Omega_v^{-1})']$ is a i.i.d. error term. For the local level, $\mu_t = \Phi\mu_{t-1} + \eta_t$, where Φ $(K \times K)$ is a parameter matrix, and $\eta_t \sim N_K(0_{K\times 1}, \Sigma_\eta) = N_K[0_{K\times 1}, \Omega_\eta^{-1}(\Omega_\eta^{-1})']$ is the multivariate i.i.d. reduced-form error term. The multivariate i.i.d. structural-form error term is $\epsilon_t = \Omega_\eta \eta_t$. Local level μ_t is initialized in the same way as for Seasonal-QVAR. Each element of the seasonality $s_t = (s_{1,t}, \ldots, s_{K,t})'$ is formulated according to the product $s_{k,t} = D_t'\rho_{k,t}$ for each $k = 1, \ldots, K$, where D_t $(S \times 1)$ is a vector of seasonal dummy variables and $\rho_{k,t}$ $(S \times 1)$ is a vector of dynamic parameters. Variable ρ_{kt} is updated according to $\rho_{k,t} = \rho_{k,t-1} + \xi_{k,t}$, where $\xi_{k,t} \sim N_S(0, \Sigma_{\xi,k})$ is a multivariate i.i.d. Gaussian error term. Variable $s_{k,t}$ is centered at zero due to the specification $\Sigma_{\xi,k} = \sigma_{\xi,k}(I_S - i_S i_S'/S)$, where $\sigma_{\xi,k}$ is a positive parameter and i_S denotes a $S \times 1$ vector of ones. Variable $\rho_{k,t}$ is initialized by using the same first-step NLS procedure that is used for Seasonal-QVAR. For the basic structural model, the following VMA(∞) representation of local level μ_t is used: $\mu_t = \sum_{j=0}^{\infty} \Phi^j \Omega_\eta^{-1} \epsilon_{t-j}$. Let C_1 denote the maximum modulus of eigenvalues of Φ. If $C_1 < 1$, then $\text{IRF}_{j,t} = \partial\mu_{t+j}/\partial\epsilon_t = \Phi^j\Omega_\eta^{-1}$ for $j = 0, 1, \ldots, \infty$. The basic structural model is estimated by using the ML method, for which the likelihood function is computed by using the Kalman filtering technique (Kalman, 1960; Harvey, 1989).

5. Data

Monthly time series data are used from world crude oil production growth $y_{1,t}$, and US IP growth $y_{2,t}$, for the period of March 1973 to April 2019.

Data on world crude oil production are from two sources. First, the book of Kilian and Lütkepohl (2017) reports data for the period of February 1973 to December 2007. Second, those data are also reported in Bloomberg (ticker: DWOPWRLD Index) for the period of February 1994 to April 2019. To validate the use of data from both sources, the correlation coefficient of world crude oil production growths from both datasets is estimated. For the correlation analysis the data period that is available from both sources is used: from January 2001 to December 2007; 83 observations from each variable. The correlation coefficient estimate is 0.9942, thus the two time series practically coincide for the period of 2001 to 2007. Motivated by this result, from February 1994, the second dataset is used for world crude oil production.

Data on the non-seasonally adjusted total US industrial production growth are from the Organi-

sation for Economic Co-operation and Development, OECD). The variable from OECD is measured in an index, based on a reference period that indicates change in the volume of production output. Due to this way of measurement, total US industrial production expresses real terms of measurement, hence, correction with respect to the consumer price index is not necessary. The importance of the industrial production is highlighted by the fact that it is one of the measures that are considered by the Business Cycle Dating Committee of the National Bureau of Economic Research (NBER), in order to establish dates of turning points in the US economy. Although several developed economies in the world, including the US, have become service sector oriented and the contribution of industrial production to the overall economic output has reduced, the importance of industrial production has not diminished in absolute terms (US Bureau of Labor Statistics). The manufacturing and construction sectors, as major economic sectors, provide a substantial amount of employment in the US economy, in which during July 2019, 12.864 million persons (8.49% of all non-farm employees) were employed in the manufacturing sector and 7.505 million persons (4.96% of all non-farm employees) were employed in the construction sector (US Bureau of Labor Statistics). An increase or decrease in the industrial output, therefore, is a sign of a strengthening or weakening of the US economy.

In this paper, $y_t = (y_{1,t}, y_{2,t})'$ (thus, for all multivariate models $K = 2$), and the seasonal dummies $D_t = (D_{\text{Jan},t}, \ldots, D_{\text{Dec},t})'$ are also used (thus, for all models, the period of the annual seasonality is $S = 12$). For $y_{1,t}$ and $y_{2,t}$, descriptive statistics and ADF with constant test results are reported in Table 1. Heteroskedasticity and autocorrelation consistent (HAC) ordinary least squares (OLS) estimates (Newey and West, 1987) of a linear regression of $y_{1,t}$ and $y_{2,t}$ on the monthly dummies are also reported in Table 1, which suggest that both variables may have seasonality components. Motivated by the work of Kilian and Lütkepohl (2017, Chapter 12.13.1), all multivariate dynamic models of the dataset used in this paper are recursively identified. Therefore, Σ_v for Seasonal-QVAR and Seasonal-VARMA is decomposed according to the Cholesky decomposition. Similarly, Σ_v and Σ_η for the basic structural model are also decomposed according to the Cholesky decomposition.

6. Results for Seasonal-QVAR and classical models

In this section, the ML estimation results are reported for Seasonal-QVAR, the basic structural model and Gaussian Seasonal-VARMA. Consistency and asymptotic normality of the ML estimates are supported by C_1 for the basic structural models and Seasonal-VARMA and the asymptotic properties of ML are also supported by C_1, C_2, C_3 or C_4 for Seasonal-QVAR (Table 2). The Escanciano and Lobato

(2009) martingale difference sequence (MDS) test is also performed for v_t and u_t of Seasonal-QVAR, and the same MDS test is performed for v_t of the basic structural model and Seasonal-VARMA. MDS is never rejected for the basic structural model and Seasonal-VARMA (Table 2). For Seasonal-QVAR, MDS is rejected for $v_{2,t}$ (Table 2), at the 10% level of significance. This diagnostic test result indicates that Seasonal-QVAR might be improved, which is investigated in Section 7.

Statistical performances are compared by using the LL, Akaike information criterion (AIC), Bayesian information criterion (BIC) and Hannan–Quinn criterion (HQC) metrics. Those metrics indicate a clear improvement in the model performance of Seasonal-QVAR, with respect to the basic structural model and Seasonal-VARMA (Table 2). It is noteworthy that Seasonal-QVAR is also estimated by using the order of variables $(y_{2,t}, y_{1,t})'$, to study the importance of the following restriction of contemporaneous effects in Table 2: US industrial production growth $\nrightarrow$ world crude oil production growth. The corresponding LL estimate is -2.6396, which is lower than the LL estimate of Table 2 for Seasonal-QVAR (i.e. -2.5386) and supports the order of variables in Table 2.

The range of local level estimates $\mu_{1,t}$ and $\mu_{2,t}$ is lower for Seasonal-QVAR than for the Gaussian alternatives (Figs. 1 to 3). This suggests that extreme observations in many cases appear in the reduced-form error term of Seasonal-QVAR instead of in the local level component, while extreme observations in many cases appear in the local level components of the basic structural model and Seasonal-VARMA instead of in the reduced-form error term (for example, compare the local level estimates for the period of the 2008 US financial crisis). The estimates of $s_{1,t}$ and $s_{2,t}$ in Figs. 1 to 3 indicate significant seasonality effects with dynamic amplitude for all models, which support the use of stochastic seasonality. Those figures indicate that extreme observations influence the seasonality components of the basic structural model and Seasonal-VARMA, while those extreme observations do not appear in the seasonality component of Seasonal-QVAR.

For Seasonal-QVAR, the score function $u_t = (u_{1,t}, u_{2,t})'$ discounts extreme values from the structural-form error term $\epsilon_t = (\epsilon_{1,t}, \epsilon_{2,t})'$. In Fig. 4, each element of the updating vector $u_t = (u_{1,t}, u_{2,t})'$ of Seasonal-QVAR is presented, as a function of $\epsilon_{1,t}$ and $\epsilon_{2,t}$. This figure indicates that both elements of the score function converge to finite values, when either of $|\epsilon_{1,t}|$ or $|\epsilon_{2,t}|$ goes to infinity. Thus, for Seasonal-QVAR, the score function discounts the influence of extreme values in the noise. To compare the discounting property of the updating terms for Seasonal-QVAR and Seasonal-VARMA, in Fig. 4 each element of the updating vector $v_t = (v_{1,t}, v_{2,t})'$ of Seasonal-VARMA is also presented, as a function

of $\epsilon_{1,t}$ and $\epsilon_{2,t}$. This figure indicates that $v_{1,t}$ and $v_{2,t}$ converge to infinity, when $|\epsilon_{1,t}|$ and $|\epsilon_{2,t}|$ go to infinity. Thus, for Seasonal-VARMA, the influence of extreme values in the noise is not discounted.

The IRF estimates for Seasonal-QVAR, the basic structural model and Seasonal-VARMA are presented in Fig. 5. The ADF tests for the elements of Q_t support the estimation of the IRFs for Seasonal-QVAR (Table 2). The signs of the IRF estimates coincide for Seasonal-QVAR, the basic structural model and Seasonal-VARMA. The following dynamic interaction effects can be highlighted in Fig. 5: US industrial production growth $\epsilon_{2,t} \longrightarrow$ world crude oil production growth $\mu_{1,t+j}$ for $j = 0, 1, \ldots, 20$. The estimates of those effects are higher for the basic structural model and Seasonal-VARMA than for Seasonal-QVAR. Given the LL-based superiority of Seasonal-QVAR, the IRF estimates suggest that the basic structural model and Seasonal-VARMA overestimate the dynamic effects of US industrial production growth on the world crude oil production growth variable. It is also shown in Fig. 5 that Seasonal-QVAR describes a lower, more precise effect than the basic structural model and Seasonal-VARMA models for the effect of US industrial production growth on crude oil production growth.

For the dynamic interaction effects of world crude oil production growth $\epsilon_{1,t} \longrightarrow$ US industrial production growth $\mu_{2,t+j}$ for $j = 0, 1, \ldots, 20$, the estimates suggest that those effects are higher and more persistent for Seasonal-QVAR than for the basic structural model and Seasonal-VARMA (Fig. 5). Seasonal-QVAR indicates a significant positive and persistent effect of crude oil production growth on US industrial production growth. The short-term effect of world crude oil production growth on US industrial production growth is proportionally more intense than the effect of US industrial production growth on world crude oil production growth. From the body of the relevant literature, the IRF estimates of the world crude oil production $\rightarrow$ US industrial production growth relation are not consistent with our results for Seasonal-QVAR. Baumeister and Peersman (2013) use data from global oil production, real acquisition cost of imported crude oil of US refineries, US real gross domestic product (GDP) and US consumer prices for the period of 1974:Q1 to 2011:Q1. IRF for oil supply shocks on real GDP is negative in that paper, in contrast with Seasonal-QVAR. Baumeister and Hamilton (2017) use data from world crude oil production, world industrial production, real crude oil price and world crude oil stock for the period of January 1958 to December 2016. IRF for oil supply shocks on world industrial production is negative in that paper, in contrast with Seasonal-QVAR. Kilian and Lütkepohl (2017) use data from world crude oil production, a business cycle index (that measures global real economic activity) and real price of oil for the period of February 1973 to December 2017.

IRF for oil supply shocks over real economic activity is non-significant in that paper, in contrast with Seasonal-QVAR. While the variables, the observation periods and the econometric models of the works of Baumeister and Peersman (2013), Baumeister and Hamilton (2017) and Kilian and Lütkepohl (2017) are different from those of the present paper, the very different IRF results and the not-completely-satisfactory model diagnostics for Seasonal-QVAR motivate an extension of Seasonal-QVAR in the following section.

7. Robustness analysis

7.1. Markov-switching (MS) models

In this section, two-regime MS models are used for y_t, where the time-varying parameters of the model are driven by an underlying Markov chain $(r_1, \ldots, r_T)$ with $r_t \in \{1, 2\}$ for $t = 1, \ldots, T$. The two-regime MS models of this paper can be extended to multi-regime MS models in a straightforward way. The evolution of r_t is modeled by using the following time-constant transition matrix:

$$P = \begin{bmatrix} \Pr(r_t = 1|r_{t-1} = 1) & \Pr(r_t = 2|r_{t-1} = 1) \\ \Pr(r_t = 1|r_{t-1} = 2) & \Pr(r_t = 2|r_{t-1} = 2) \end{bmatrix} = \begin{pmatrix} p & 1-p \\ 1-q & q \end{pmatrix} \tag{10}$$

where p and q are the constant transition probability parameters. The Markov chain $(r_1, \ldots, r_T)$ is stationary with time-invariant probabilities $\pi^*(1) = \Pr(r_t = 1) = (1-q)/(2-p-q)$ and $\pi^*(2) = 1-\pi^*(1)$. The following filtered probabilities of regimes are also defined: $\pi_t(1) = \Pr(r_t = 1|y_1, \ldots, y_{t-1})$ and $\pi_t(2) = \Pr(r_t = 2|y_1, \ldots, y_{t-1})$, and $\tilde{\pi}_t(1) = \Pr(r_t = 1|y_1, \ldots, y_t)$ and $\tilde{\pi}_t(2) = \Pr(r_t = 2|y_1, \ldots, y_t)$. These filtered probabilities are computed recursively for $t = 1, \ldots, T$:

$$\begin{aligned} \pi_t(1) &= p\tilde{\pi}_{t-1}(1) + (1-q)\tilde{\pi}_{t-1}(2) \\ \pi_t(2) &= 1 - \pi_t(1) \\ \tilde{\pi}_t(1) &= \frac{f(y_t|y_1,\ldots,y_{t-1},r_t=1;\Theta)\pi_t(1)}{f(y_t|y_1,\ldots,y_{t-1},r_t=1;\Theta)\pi_t(1)+f(y_t|y_1,\ldots,y_{t-1},r_t=2;\Theta)\pi_t(2)} \\ \tilde{\pi}_t(2) &= 1 - \tilde{\pi}_t(1) \end{aligned} \tag{11}$$

where $f(y_t|y_1, \ldots, y_{t-1}, r_t; \Theta)$ denotes the regime-dependent conditional density of the dependent variable in MS-Seasonal-QVAR, and $\tilde{\pi}_0(1) = \pi^*(1)$ and $\tilde{\pi}_0(2) = \pi^*(2)$ are used for initialization. Given the parameter estimates of MS-Seasonal-QVAR, statistical inferences on r_t are also made by using the smoothed probability $\Pr(r_t|y_1, \ldots, y_T)$, according to the following algorithm of Kim and Nelson (1999).

For each period t, the smoothed probabilities of regimes are given by:

$$\Pr(r_t = j|y_1, \ldots, y_T) = \sum_{k=1,2} \Pr(r_t = j, r_{t+1} = k|y_1, \ldots, y_T) \tag{12}$$

where

$$\Pr(r_t = j, r_{t+1} = k|y_1, \ldots, y_T) \simeq \frac{\Pr(r_{t+1} = k|y_1, \ldots, y_T) \Pr(r_{t+1} = k|r_t = j)\tilde{\pi}_t(j)}{\pi_{t+1}(k)} \tag{13}$$

for $j = 1, 2$ and $k = 1, 2$. The smoothed probabilities of regimes are computed recursively for $t = T, \ldots, 1$. The recursion is started at $t = T$, by using the ML estimates of p, q, $\pi_T(k)$ and $\tilde{\pi}_T(k)$.

7.2. MS-Seasonal-QVAR

MS-Seasonal-QVAR is able to separate different regimes in the data, due to the outlier-discounting property of the score functions that update the dynamic equations. For classical models from the time series literature, such as ARMA, GARCH or VAR, the separation of different regimes may be difficult, as those models are sensitive to outliers. For example, MS-GARCH may switch to a different regime after each extreme observation, and it may identify more switches in regimes than MS-Beta-t-EGARCH (Blazsek and Ho, 2017) or other MS score-driven volatility specifications (Blazsek et al., 2018). Alternatives to the MS approach for multivariate models are the vector threshold autoregressive (VTAR) models and the vector smooth transition autoregressive (VSTAR) models (Hubrich and Teräsvirta, 2013); score-driven versions of VTAR and VSTAR may be introduced in future works.

For y_t $(K \times 1)$ with $t = 1, \ldots, T$, MS-Seasonal-QVAR is $y_t = c(r_t) + \mu_t(r_t) + s_t(r_t) + v_t(r_t)$, where $c(r_t)$ $(K \times 1)$ is the vector of constant parameters, $\mu_t(r_t)$ $(K \times 1)$ is the local level component, $s_t(r_t)$ $(K \times 1)$ is the seasonality component, and $v_t(r_t)$ $(K \times 1)$ is the reduced-form error term. In the MS-Seasonal-QVAR specification of this paper, all components of y_t depend on the contemporaneous value of the regime variable r_t. The reduced-form error term $v_t(r_t)$ is specified as multivariate i.i.d. $v_t(r_t) \sim t_K[0, \Sigma_v(r_t), \nu(r_t)]$, where $\Sigma_v(r_t) = \Omega_v^{-1}(r_t)[\Omega_v^{-1}(r_t)]'$ is the positive definite regime-dependent scaling matrix and $\nu(r_t) > 2$ is the regime-dependent degrees of freedom parameter. As a consequence, $E[v_t(r_t)] = 0$ and $\text{Var}[v_t(r_t)] = \Sigma_v(r_t) \times \nu(r_t)/[\nu(r_t) - 2]$. Moreover, the multivariate i.i.d. structural-form error term is $\epsilon_t(r_t) = \{\nu(r_t)/[\nu(r_t)-2]\}^{-1/2}\Omega_v(r_t) \times v_t(r_t)$, for which $E[\epsilon_t(r_t)] = 0$ and $\text{Var}[\epsilon_t(r_t)] =$

I_K. The log of the regime-dependent conditional density of y_t is

$$\ln f(y_t|y_1,\ldots,y_{t-1},r_t;\Theta) = \ln\Gamma\left[\frac{\nu(r_t)+K}{2}\right] - \ln\Gamma\left[\frac{\nu(r_t)}{2}\right] - \frac{K}{2}\ln[\pi\nu(r_t)] \tag{14}$$

$$-\frac{1}{2}\ln|\Sigma_v(r_t)| - \frac{\nu(r_t)+K}{2}\ln\left[1+\frac{v_t(r_t)'\Sigma_v(r_t)^{-1}v_t(r_t)}{\nu(r_t)}\right]$$

The regime-dependent score function with respect to $\mu_t(r_t)$ is

$$\frac{\partial \ln f(y_t|y_1,\ldots,y_{t-1},r_t;\Theta)}{\partial\mu_t(r_t)} = \frac{\nu(r_t)+K}{\nu(r_t)}\Sigma_v^{-1}(r_t)\times\left[1+\frac{v_t'(r_t)\Sigma_v^{-1}(r_t)v_t(r_t)}{\nu(r_t)}\right]^{-1}v_t(r_t) \tag{15}$$

Based on this equation, the $(K\times 1)$ regime-dependent scaled score function vector is defined as:

$$u_t(r_t) = \left[1+\frac{v_t'(r_t)\Sigma_v^{-1}(r_t)v_t(r_t)}{\nu(r_t)}\right]^{-1}v_t(r_t) \tag{16}$$

The local level component is $\mu_t(r_t) = \Phi(r_t)\mu_{t-1}(r_t) + \Psi(r_t)u_{t-1}(r_t)$ where where $\Phi(r_t)$ $(K\times K)$ and $\Psi(r_t)$ $(K\times K)$ are regime-dependent parameter matrices, and define the variables: $\mu_{t-1}(r_t) = E[\mu_{t-1}(r_{t-1})|y_1,\ldots,y_{t-1},r_t]$ and $u_{t-1}(r_t) = E[u_{t-1}(r_{t-1})|y_1,\ldots,y_{t-1},r_t]$. These expectations are computed with respect to r_{t-1} (Appendix B). Therefore, the updating terms of $\mu_t(r_t)$ depend only on the contemporaneous regime variable, which simplifies the statistical inference. This non-path-dependent updating is based on the works of Gray (1996) and Klaassen (2002), where a similar updating mechanism for the MS-GARCH model was used. Local level $\mu_t(r_t)$ is initialized by using $\mu_1(r_t) = 0_{K\times 1}$.

The seasonality component $s_t(r_t) = [s_{1,t}(r_t),\ldots,s_{K,t}(r_t)]'$ is formulated according to $s_{k,t}(r_t) = D_t'\rho_{k,t}(r_t)$ for each $k = 1,\ldots,K$, where $D_t = (D_{1,t},\ldots,D_{S,t})'$ is a vector of seasonal dummy variables and $\rho_{k,t}(r_t) = [\rho_{k,1,t}(r_t),\ldots,\rho_{k,S,t}(r_t)]'$ is a vector of dynamic seasonality parameters. Variable $\rho_{k,t}(r_t)$ is updated according to $\rho_{k,t}(r_t) = \rho_{k,t-1}(r_t) + \gamma_{k,t}(r_t)u_{k,t-1}(r_t)$, where $\gamma_{k,t}(r_t) = [\gamma_{k,1,t}(r_t),\ldots,\gamma_{k,S,t}(r_t)]'$ is a dynamic scaling parameter, and $\rho_{k,t-1}(r_t) = E[\rho_{k,t-1}(r_{t-1})|y_1,\ldots,y_{t-1},r_t]$ (Appendix B). Moreover, $u_{k,t-1}(r_t)$ is the k-th element of $u_{t-1}(r_t)$ that is defined in the same way as for $\mu_t(r_t)$ (Appendix B). Each element of $\gamma_{k,t}(r_t)$ is given by $\gamma_{k,j,t}(r_t) = \gamma_{k,j}(r_t)$ for $D_{j,t} = 1$ and $\gamma_{k,j,t}(r_t) = -\gamma_{k,j}(r_t)/(S-1)$ for $D_{j,t} = 0$, where $\gamma_{k,j}(r_t)$ with $j = 1,\ldots,S$ are seasonality parameters to be estimated. This parameterization ensures that $\sum_{j=1}^{S}\gamma_{k,j,t}(r_t) = 0$ for each regime. Variable $\rho_{k,t}(r_t)$ is initialized by using a first-step NLS procedure, in which $y_{k,t}$ is regressed on the seasonal dummy variables.

7.3. IRFs

The regime-dependent IRFs are considered in this paper. First, the regime-dependent structural-form nonlinear VMA(∞) representation of $\mu_t(r_t)$ is:

$$\mu_t(r_t) = \sum_{j=0}^{\infty} \Phi^j(r_t)\Psi(r_t)\{[\nu(r_t)-2]\nu(r_t)\}^{1/2}\Omega_v^{-1}(r_t)\frac{\epsilon_{t-1-j}(r_{t-1-j})}{\nu(r_t)-2+\epsilon_{t-1-j}(r_{t-1-j})'\epsilon_{t-1-j}(r_{t-1-j})} \quad (17)$$

The maximum modulus of eigenvalues of $\Phi(r_t)$ for $r_t = 1, 2$ is denoted by $C_1(r_t)$. If $C_1(r_t) < 1$ for $r_t = 1, 2$, then the series in Equation (17) is convergent. The regime-dependent $\text{IRF}_{j,t}(r_t)$ is:

$$\text{IRF}_{j,t}(r_t) = \frac{\partial \mu_{t+j}(r_{t+j})}{\partial \epsilon_{t-1}(r_{t-1})} = \Phi^j(r_t)\Psi(r_t)\{[\nu(r_t)-2]\nu(r_t)\}^{1/2}\Omega_v^{-1}(r_t)Q_{t-1-j}(r_{t-1-j}) \quad (18)$$

for $j = 0, 1, \ldots, \infty$, where

$$Q_t(r_t) = \frac{\partial \frac{\epsilon_t(r_t)}{\nu(r_t)-2+\epsilon_t'(r_t)\epsilon_t(r_t)}}{\partial \epsilon_t(r_t)} = \begin{bmatrix} q_{1,1,t}(r_t) & \cdots & q_{1,K,t}(r_t) \\ \cdots & \cdots & \cdots \\ q_{K,1,t}(r_t) & \cdots & q_{K,K,t}(r_t) \end{bmatrix} = \quad (19)$$

$$= \begin{bmatrix} \frac{\nu(r_t)-2+\epsilon_t(r_t)'\epsilon_t(r_t)-2\epsilon_{1,t}(r_t)^2}{[\nu(r_t)-2+\epsilon_t(r_t)'\epsilon_t(r_t)]^2} & \frac{-2\epsilon_{1,t}(r_t)\epsilon_{2,t}(r_t)}{[\nu(r_t)-2+\epsilon_t'(r_t)\epsilon_t(r_t)]^2} & \cdots & \frac{-2\epsilon_{1,t}(r_t)\epsilon_{K,t}(r_t)}{[\nu(r_t)-2+\epsilon_t'(r_t)\epsilon_t(r_t)]^2} \\ \frac{-2\epsilon_{2,t}(r_t)\epsilon_{1,t}(r_t)}{[\nu(r_t)-2+\epsilon_t'(r_t)\epsilon_t(r_t)]^2} & \frac{\nu(r_t)-2+\epsilon_t'(r_t)\epsilon_t(r_t)-2\epsilon_{2,t}(r_t)^2}{[\nu(r_t)-2+\epsilon_t'(r_t)\epsilon_t(r_t)]^2} & \cdots & \cdots \\ \cdots & \cdots & \cdots & \cdots \\ \frac{-2\epsilon_{K,t}(r_t)\epsilon_{1,t}(r_t)}{[\nu(r_t)-2+\epsilon_t'(r_t)\epsilon_t(r_t)]^2} & \cdots & \cdots & \frac{\nu(r_t)-2+\epsilon_t'(r_t)\epsilon_t(r_t)-2\epsilon_{K,t}^2(r_t)}{[\nu(r_t)-2+\epsilon_t(r_t)'\epsilon_t(r_t)]^2} \end{bmatrix}$$

for $r_t = 1, 2$. The IRFs are time-varying for MS-QVAR for $r_t = 1, 2$, due to $Q_{t-1-j}(r_{t-1-j})$. In this paper, the following regime-dependent unconditional mean of $\text{IRF}_{j,t}(r_t)$ is used:

$$\text{IRF}_j(r_t) = E[\text{IRF}_{j,t}(r_t)] = \Phi^j(r_t)\Psi\{[\nu(r_t)-2]\nu(r_t)\}^{1/2}\Omega_v^{-1}(r_t)E[Q_{t-1-j}(r_{t-1-j})] \quad (20)$$

for $j = 0, 1, \ldots, \infty$ and $r_t = 1, 2$. The expected value $E[Q_{t-1-j}(r_{t-1-j})]$ is estimated by using the sample average of $Q_t(r_t)$ for $r_t = 1, 2$, which is supported by the ADF test with constant.

7.4. Statistical inference of MS-Seasonal-QVAR

Seasonal-QVAR is estimated numerically by using the maximum likelihood (ML) method:

$$\hat{\Theta}_{\mathrm{ML}} = \arg\max_{\Theta} \mathrm{LL}(y_1, \ldots, y_T; \Theta) = \arg\max_{\Theta} \sum_{t=1}^{T} \sum_{i=1}^{2} \ln[\pi_t(i) f(y_t | y_1, \ldots, y_{t-1}, r_t = i; \Theta)] \tag{21}$$

where $f(y_t|y_1, \ldots, y_{t-1}, r_t; \Theta)$ is the exponential of Equation (14). Numerical maximization of LL and estimation of standard errors of Θ are performed in the same way as for Seasonal-QVAR.

Although MS-Seasonal-QVAR is new in the literature on DCS models, several technical aspects of the statistical inference of MS-Seasonal-QVAR are in relation to the MS-VAR model (Krolzig, 1997). We also refer to the work of Abramson and Cohen (2007), which presents conditions of the asymptotic properties of the ML estimator for different MS-GARCH specifications. The proofs of those conditions are in relation to the proofs of the ML conditions for MS-Seasonal-QVAR in this paper, which ensure the covariance stationarity of $\mu_t(r_t)$ and the consistent estimation of the corresponding elements of the information matrix. For the parameters in $s_t(r_t)$, the conditions of ML are satisfied, because the parameter matrix of $\rho_{k,t-1}(r_t)$ is set to the identity matrix in $\rho_{k,t}(r_t) = \rho_{k,t-1}(r_t) + \gamma_{k,t}(r_t) u_{k,t-1}(r_t)$.

First, Condition 1 is the covariance stationarity of $\mu_t(r_t)$, which is expressed as:

$$\begin{aligned}
\mu_t(r_t) &= \Phi(r_t)\mu_{t-1}(r_t) + \Psi(r_t)u_{t-1}(r_t) \\
&= \Phi(r_t)E[\mu_{t-1}(r_{t-1})|y_1, \ldots, y_{t-1}, r_t] + \Psi(r_t)E[u_{t-1}(r_{t-1})|y_1, \ldots, y_{t-1}, r_t] \\
&= \Phi(r_t)\mu_{t-1}(r_{t-1} = 1)\Pr(r_{t-1} = 1|y_1, \ldots, y_{t-1}, r_t) \\
&\quad + \Phi(r_t)\mu_{t-1}(r_{t-1} = 2)\Pr(r_{t-1} = 2|y_1, \ldots, y_{t-1}, r_t) \\
&\quad + \Psi(r_t)u_{t-1}(r_{t-1} = 1)\Pr(r_{t-1} = 1|y_1, \ldots, y_{t-1}, r_t) \\
&\quad + \Psi(r_t)u_{t-1}(r_{t-1} = 2)\Pr(r_{t-1} = 2|y_1, \ldots, y_{t-1}, r_t)
\end{aligned} \tag{22}$$

To show the condition of covariance stationarity of $\mu_t(r_t)$, the conditional mean $E[\mu_t(r_t)|y_1, \ldots, y_{t-1}, r_t]$ is evaluated for both sides of Equation (22), from which we consider the following terms:

$$\begin{aligned}
&E[\mu_{t-1}(r_{t-1})\Pr(r_{t-1}|y_1, \ldots, y_{t-1}, r_t)|y_1, \ldots, y_{t-1}, r_t] \\
&= \textstyle\int_{\{y_1,\ldots,y_{t-1}\}} \mu_{t-1}(r_{t-1})\Pr(r_{t-1}|y_1, \ldots, y_{t-1}, r_t) g(y_1, \ldots, y_{t-1}|r_t) d(y_1, \ldots, y_{t-1}) \\
&= \textstyle\int_{\{y_1,\ldots,y_{t-1}\}} \mu_{t-1}(r_{t-1})\Pr(r_{t-1}|r_t) g(y_1, \ldots, y_{t-1}|r_{t-1}, r_t) d(y_1, \ldots, y_{t-1}) \\
&= \Pr(r_{t-1}|r_t) E[\mu_{t-1}(r_{t-1})|y_1, \ldots, y_{t-2}, r_{t-1}]
\end{aligned} \tag{23}$$

$$
\begin{aligned}
&E[u_{t-1}(r_{t-1})\Pr(r_{t-1}|y_1,\ldots,y_{t-1},r_t)|y_1,\ldots,y_{t-1},r_t] \\
&= \textstyle\int_{\{y_1,\ldots,y_{t-1}\}} u_{t-1}(r_{t-1})\Pr(r_{t-1}|y_1,\ldots,y_{t-1},r_t)g(y_1,\ldots,y_{t-1}|r_t)d(y_1,\ldots,y_{t-1}) \\
&= \textstyle\int_{\{y_1,\ldots,y_{t-1}\}} u_{t-1}(r_{t-1})\Pr(r_{t-1}|r_t)g(y_1,\ldots,y_{t-1}|r_{t-1},r_t)d(y_1,\ldots,y_{t-1}) \\
&= \Pr(r_{t-1}|r_t)E[u_{t-1}(r_{t-1})|y_1,\ldots,y_{t-2},r_{t-1}]
\end{aligned}
\tag{24}
$$

where g is a joint density function and the value of r_{t-1} is not specified as the expectation is with respect to $\{y_1,\ldots,y_{t-1}\}$. Thus, $E[\mu_t(r_t)|y_1,\ldots,y_{t-1},r_t]$ can be recursively constructed:

$$
\begin{aligned}
E[\mu_t(r_t)|y_1,\ldots,y_{t-1},r_t] \;=\; & \Phi(r_t)\Pr(r_{t-1}|r_t)E[\mu_{t-1}(r_{t-1})|y_1,\ldots,y_{t-2},r_{t-1}] \\
& +\Psi(r_t)\Pr(r_{t-1}|r_t)E[u_{t-1}(r_{t-1})|y_1,\ldots,y_{t-2},r_{t-1}]
\end{aligned}
\tag{25}
$$

The probability $\Pr(r_{t-1}|r_t)$ in Equation (25) for $r_t = 1,2$ and $r_{t-1} = 1,2$ is given by:

$$
\begin{aligned}
&\Pr(r_{t-1}=1|r_t=1) = \Pr(r_t=1|r_{t-1}=1) = p \\
&\Pr(r_{t-1}=2|r_t=1) = \tfrac{\pi^*(2)}{\pi^*(1)}\Pr(r_t=1|r_{t-1}=2) = \tfrac{\pi^*(2)}{\pi^*(1)}(1-q) \\
&\Pr(r_{t-1}=1|r_t=2) = \tfrac{\pi^*(1)}{\pi^*(2)}\Pr(r_t=2|r_{t-1}=1) = \tfrac{\pi^*(1)}{\pi^*(2)}(1-p) \\
&\Pr(r_{t-1}=2|r_t=2) = \Pr(r_t=2|r_{t-1}=2) = q
\end{aligned}
\tag{26}
$$

Based on Equations (25) and (26) and by considering all possible values of r_t and r_{t-1} in Equation (25), the following matrix is defined:

$$
\begin{bmatrix}
\Phi(1)p & \Phi(1)\frac{\pi^*(2)}{\pi^*(1)}(1-q) \\
\Phi(2)\frac{\pi^*(1)}{\pi^*(2)}(1-p) & \Phi(2)q
\end{bmatrix}
\tag{27}
$$

If the maximum modulus of eigenvalues, C_1, of this matrix is less than one, then Condition 1 is satisfied.

Second, Condition 2, denoted as C_2, holds if $E[u_{j,t-1}^{2-i}(r_t)[\partial u_{k,t-1}(r_t)/\partial\mu_{l,t-1}(r_t)]^i] < \infty$, where $i = 0,1,2$, $j,k,l = 1,\ldots,K$ for $r_t = 1,2$, and define the derivative of the score function as:

$$
\frac{\partial u_{k,t-1}(r_t)}{\partial\mu_{l,t-1}(r_t)} = E\left[\frac{\partial u_{k,t-1}(r_{t-1})}{\partial\mu_{l,t-1}(r_{t-1})}|y_1,\ldots,y_{t-1},r_t\right]
\tag{28}
$$

For Condition 2 the sample average estimator is used that is supported by the ADF test with constant.

Third, for Condition 3 the derivative of the local level $\mu_t(r_t)$ with respect to $\Psi_{i,j}(r_t)$ is:

$$\frac{\partial \mu_t(r_t)}{\partial \Psi_{i,j}(r_t)} = \left[\Phi(r_t) + \Psi(r_t)\frac{\partial u_{t-1}(r_t)}{\partial \mu'_{t-1}(r_t)}\right]\frac{\partial \mu_{t-1}(r_t)}{\partial \Psi_{i,j}(r_t)} + W_{i,j}u_{t-1}(r_t) = X_t(r_t)\frac{\partial \mu_{t-1}(r_t)}{\partial \Psi_{i,j}(r_t)} + W_{i,j}u_{t-1}(r_t) \quad (29)$$

for all $t = 1, \ldots, T$, where the element (i, j) of the matrix $W_{i,j}$ $(K \times K)$ is one and the rest of the elements of $W_{i,j}$ are zero. For Condition 3, the same arguments as for Condition 1 are used in Equation (29). Thus, the following matrix is defined:

$$\left\{ \begin{array}{ll} E[X_t(1)]p & E[X_t(1)]\frac{\pi^*(2)}{\pi^*(1)}(1-q) \\ E[X_t(2)]\frac{\pi^*(1)}{\pi^*(2)}(1-p) & E[X_t(2)]q \end{array} \right\} \quad (30)$$

If the maximum modulus of eigenvalues, C_3, of this matrix is less than one, then Condition 3 is satisfied.

Fourth, for Condition 4, the regime-dependent information matrix depends on:

$$\begin{aligned} &\text{vec}\left[\frac{\partial \mu_t(r_t)}{\partial \Psi_{i,j}(r_t)}\frac{\partial \mu'_t(r_t)}{\partial \Psi_{k,l}(r_t)}\right] = [X_t(r_t) \otimes X_t(r_t)]\text{vec}\left[\frac{\partial \mu_{t-1}(r_t)}{\partial \Psi_{i,j}(r_t)}\frac{\partial \mu'_{t-1}(r_t)}{\partial \Psi_{k,l}(r_t)}\right] \quad (31) \\ &+\text{vec}\left[X_t(r_t)\frac{\partial \mu_{t-1}(r_t)}{\partial \Psi_{i,j}(r_t)}W'_{i,j}u_{t-1}(r_t)\right] + \text{vec}\left[u'_{t-1}(r_t)W_{k,l}\frac{\partial \mu'_{t-1}(r_t)}{\partial \Psi_{k,l}(r_t)}X'_t(r_t)\right] \\ &+\text{vec}\left[W_{i,j}u_{t-1}(r_t)u'_{t-1}(r_t)W'_{k,l}\right] \end{aligned}$$

where $\otimes$ is the Kronecker product and $\text{vec}(x)$ indicates that the columns of the matrix are being stacked one upon the other. For Condition 4, the following matrix is defined:

$$\left\{ \begin{array}{ll} E[X_t(1) \otimes X_t(1)]p & E[X_t(1) \otimes X_t(1)]\frac{\pi^*(2)}{\pi^*(1)}(1-q) \\ E[X_t(2) \otimes X_t(2)]\frac{\pi^*(1)}{\pi^*(2)}(1-p) & E[X_t(2) \otimes X_t(2)]q \end{array} \right\} \quad (32)$$

If the maximum modulus of eigenvalues, C_4, of this matrix is less than one, then Condition 4 is satisfied.

7.5. Results for MS-Seasonal-QVAR

Several alternative specifications were considered for MS-Seasonal-QVAR, in which different sets of model parameters are regime-switching. In this section, results are reported for the following specifications: $c(r_t)$, $\mu_t(r_t)$, s_t, $v_t(r_t)$ and $c(r_t)$, μ_t, s_t, $v_t(r_t)$. More specific versions of MS-Seasonal-QVAR are also estimated, but the LL-based model performance metrics and the model diagnostic tests support the reported specifications. The most general specification, for which all of the parameters are

regime-switching, i.e. $c(r_t)$, $\mu_t(r_t)$, $s_t(r_t)$, $v_t(r_t)$, was not identified for the dataset of this paper.

The parameter estimates indicate highly stable regimes, as both p and q are above 99% for both reported MS-Seasonal-QVAR specifications (Table 3). The estimates of $\Omega_v^{-1}(r_t)$ (Table 3) suggest naming regime $r_t = 1$ as a high-volatility regime and naming regime $r_t = 2$ as a low-volatility regime. The degrees of freedom parameter estimates indicate that the first three and four moments are finite for the two reported specifications, respectively (Table 3). The parameter estimates also show that several parameters of $\mu_t(r_t)$ and $s_t(r_t)$ are statistically significant in both regimes and the corresponding standard error estimates clearly indicate that the values of many of those parameters are different in different regimes (Table 3).

Consistency and asymptotic normality of the ML estimates are supported by C_1, C_2, C_3 or C_4 for both specifications of MS-Seasonal-QVAR (Table 4). The Escanciano and Lobato (2009) test is also performed for the one-step prediction errors of $v_t(r_t)$ and $u_t(r_t)$. The use of the one-step prediction errors is motivated by the work of Krolzig (1997), which suggests their use for the residual-based model checking of MS-VAR. The one-step prediction errors are: $E[v_t(r_t)] = \pi_t(1)v_t(1) + \pi_t(2)v_t(2)$ and $E[u_t(r_t)] = \pi_t(1)u_t(1) + \pi_t(2)u_t(2)$. MDS is never rejected for MS-Seasonal-QVAR (Table 4), which indicates an improvement in the model specification with respect to Seasonal-QVAR. Furthermore, the LL-based model performance metrics show that the statistical performance of MS-Seasonal-QVAR (Table 4) is clearly superior to Seasonal-QVAR and the classical Gaussian multivariate alternatives (Table 2). The LL-based model selection metrics also show that MS-Seasonal-QVAR with $c(r_t)$, $\mu_t(r_t)$, s_t, $v_t(r_t)$ is superior to MS-Seasonal-QVAR with $c(r_t)$, μ_t, s_t, $v_t(r_t)$.

Motivated by the LL-based model selection metrics, the time series components of MS-Seasonal-QVAR with $c(r_t)$, $\mu_t(r_t)$, s_t, $v_t(r_t)$ are presented in Figs. 6 and 7 for the high-volatility regime ($r_t = 1$) and the low-volatility regime ($r_t = 2$), respectively. The estimates of $\mu_{1,t}(r_t)$ and $\mu_{2,t}(r_t)$ are presented in Figs. 6 and 7, respectively. Those estimates show different local level components in those regimes and graphically illustrate that $r_t = 1$ is the high-volatility regime and $r_t = 2$ is the low-volatility regime. The estimates of $s_{1,t}(r_t)$ and $s_{2,t}(r_t)$ are presented in Figs. 6 and 7, respectively, and they indicate significant seasonality effects with dynamic amplitude for all models that are different in different regimes. The estimates of filtered and smoothed probabilities for MS-Seasonal-QVAR with $c(r_t)$, $\mu_t(r_t)$, s_t, $v_t(r_t)$ indicate that both regimes are stable (Fig. 8). The figure shows that the regime switching from the high- to the low-volatility regime is during 1992. The filtered probabilities also

show that several outliers are identified by MS-Seasonal-QVAR during the sample period.

In the remainder of this section, the IRFs between world crude oil production growth $y_{1,t}$ and US industrial production growth $y_{2,t}$ are presented for the MS-Seasonal-QVAR specification with $c(r_t)$, $\mu_t(r_t)$, s_t, $v_t(r_t)$ (see Fig. 9). The IRFs start from positive effects for all cases (Fig. 9) which is similar to the other single-regime and MS specifications. Nevertheless, the positive sign changes to the negative sign for Industrial production growth of the US $\epsilon_{2,t} \longrightarrow$ Oil production growth $\mu_{1,t+j}$, in both regimes. Moreover, the positive sign changes to the negative sign for Oil production growth $\epsilon_{1,t} \longrightarrow$ Industrial production growth of the US $\mu_{2,t+j}$, in the low-volatility regime. The IRF estimates suggest that the IRF values are higher in the high-volatility regime, than in the low-volatility regime. The IRF estimates for MS-Seasonal-QVAR, with respect to the world crude oil production $\rightarrow$ US economic activity, are in relation to the results from the literature on crude oil supply shocks. Those effects are negative for the low-volatility period (from June 1992 to April 2019), which is similar to the negative IRF estimates of Baumeister and Peersman (2013) and Baumeister and Hamilton (2017). On the other hand, for the high-volatility period (from March 1973 to May 1992), the opposite positive effects are found for the same relation. The switching effects for the world crude oil production to US economic activity relation may explain why the same IRF is non-significant in the work of Kilian and Lütkepohl (2017).

8. Conclusions

The practical use of Seasonal-QVAR and MS-Seasonal-QVAR has been suggested for the estimation of dynamic interaction effects between world crude oil production growth and US industrial production growth. These models are alternatives to the classical Gaussian multivariate models, from which we have considered: (i) basic structural model that is a parameter-driven state space model, and (ii) Seasonal-VARMA that is an observation-driven model and it is the limiting special case of Seasonal-QVAR. Data from world crude oil production growth and United States industrial production have been used for the period of March 1973 to April 2019. The results have indicated that score-driven multivariate state space models provide more reliable statistical estimates than the classical models.

The filters in Seasonal-QVAR and MS-Seasonal-QVAR are robust to outliers, and MS-Seasonal-QVAR is able to identify structural changes for the sample period. For both score-driven models, several conditions of the ML estimator have been shown. All of those conditions are satisfied for MS-Seasonal-QVAR, and the corresponding IRF estimates are similar to the results of some relevant papers from the literature on crude oil supply shocks. The statistical performance of MS-Seasonal-QVAR has

been superior to the statistical performance of Seasonal-QVAR. This is due to the facts that: (i) MS-Seasonal-QVAR has identified a structural change in 1992, and (ii) MS-Seasonal-QVAR has identified several outliers in the world crude oil production growth and US industrial production growth variables. The results of the present paper have indicated that MS-Seasonal-QVAR provides more precise IRF estimates for different regimes of the data generating process than Seasonal-QVAR and the classical multivariate models, and therefore it may be an effective tool of practitioners for macroeconomic analyses. The smoothed probabilities of regimes estimates for MS-Seasonal-QVAR motivate the use of the score-driven versions of VTAR and VSTAR, as alternatives to MS-Seasonal-QVAR, for world crude oil production and US industrial production in future works.

Acknowledgments

Previous versions of this work were presented in "Recent Advances in Econometrics: International Conference in Honor of Luc Bauwens" (Brussels, October 19-20, 2017), GESG Seminar (Guatemala City, December 7, 2017), "Workshop in Time Series Econometrics" (Zaragoza, April 12-13, 2018), and "International Conference on Statistical Methods for Big Data" (Madrid, July 7-8, 2018). The authors are thankful to Luc Bauwens, Matthew Copley, Antoni Espasa, Eric Ghysels, Joachim Grammig, Andrew Harvey, Søren Johansen, Bent Nielsen, Eric Renault, Genaro Sucarrat, and Ruey Tsay. Blazsek and Licht acknowledge funding from Universidad Francisco Marroquín. Escribano acknowledges funding from the Ministry of Economics of Spain (ECO2016-00105-001, MDM 2014-0431) and the Community of Madrid (MadEco-CM S2015/HUM-3444).

References

Abramson, A., Cohen, I., 2007. On the stationarity of Markov-switching GARCH processes. Econometric Theory 23 (3): 485–500. doi: 10.1017/S0266466607070211.

Alquist, R., Kilian, L., Vigfusson, R.J., 2011. Forecasting the price of oil. Board of Governors of the Federal Reserve System, International Finance Discussion Papers, No. 1022.

Ayala, A., Blazsek, S., 2018. Score-driven currency exchange rate seasonality as applied to the Guatemalan Quetzal/US Dollar. SERIEs Journal of the Spanish Economic Association 10 (1): 65–92. doi: 10.1007/s13209-018-0186-0.

Ayala, A., Blazsek, S., 2019. Score-driven models of stochastic seasonality in location and scale: an application case study of the Indian Rupee to USD exchange rate. Applied Economics 51 (37): 4083–4103. doi: 10.1080/00036846.2019.1588952.

Ayala, A., Blazsek, S., Escribano, A., 2019. Maximum likelihood estimation of score-driven models with dynamic shape parameters: an application to Monte Carlo value-at-risk. Working Paper 19-12, University Carlos III of Madrid,

Department of Economics. https://e-archivo.uc3m.es/handle/10016/28638.

Balke, N.S., Fomby, T.B., 1994. Large shocks, small shocks, and economic fluctuations: outliers in macroeconomic time series. Journal of Applied Econometrics 9 (2): 181–200. doi: 10.1002/jae.3950090205.

Barsky, R.B., Kilian, L., 2002. Do we really know that oil caused the Great Stagflation? A monetary alternative (pp. 137–183). In: B.S. Bernanke and K. Rogoff, eds., NBER Macroeconomics Annual 2001. MIT Press, Cambridge.

Barsky, R.B., Kilian, L., 2004. Oil and the macroeconomy since the 1970s. Journal of Economic Perspectives 18 (4): 115–134. doi: 10.1257/0895330042632708.

Baumeister, C., Peersman, G., 2013. Time-varying effects of oil supply shocks on the US economy. American Economic Journal: Macroeconomics 5 (4): 1–28. doi: 10.1257/mac.5.4.1.

Baumeister, C., Kilian, L., 2014. What central bankers need to know about forecasting oil prices. International Economic Review 55 (3): 869–889. doi: 10.1111/iere.12074.

Baumeister, C.J.S., Hamilton, J.D., 2017. Structural interpretation of vector autoregressions with incomplete identification: revisiting the role of oil supply and demand shocks. NBER Working Paper, No. 24167.

Baxter, M., King, R.G., 1999. Measuring business cycles: approximate band-pass filter for economic time series. The Review of Economics and Statistics 81 (4): 575–593. doi: 10.1162/003465399558454.

Bernanke, B.S., Gertler, M., Watson, M., 1997. Systematic monetary policy and the effects of oil price shocks. Brookings Papers on Economic Activity 1: 91–157. doi: 10.2307/2534702.

Blanchard, O.J., 2002. Comments on 'Do we really know that oil caused the Great Stagnation? A monetary alternative' by Robert Barsky and Lutz Kilian (pp. 183–192). In: B. Bernanke and K. Rogoff, eds., NBER Macroeconomics Annual. MIT Press, Cambridge.

Blanchard, O.J., Riggi, M., 2013. Why are the 2000s so different from the 1970s? A structural interpretation of changes in the macroeconomic effects of oil. Journal of the European Economic Association 11 (5): 1032–1052. doi: 10.1111/jeea.12029.

Blasques, F., Koopman, S.J., Lucas, A., 2015. Information-theoretic optimality of observation-driven time series models for continuous responses. Biometrika 102 (2): 325–343. doi: 10.1093/biomet/asu076.

Blazsek, S., Escribano, A., 2010. Knowledge spillovers in U.S. patents: a dynamic patent intensity model with secret common innovation factors. Journal of Econometrics 159 (1): 14–32. doi: 10.1016/j.jeconom.2010.04.004.

Blazsek, S., Escribano, A., 2016. Patent propensity, R&D and market competition: dynamic spillovers of innovation leaders and followers. Journal of Econometrics 191 (1): 145–163. doi: 10.1016/j.jeconom.2015.10.005.

Blazsek, S., Escribano, A., 2016. Score-driven dynamic patent count panel data models. Economics Letters 149 (C): 116–119. doi: 10.1016/j.econlet.2016.10.026.

Blazsek, S., Escribano, A., Licht, A., 2019. Co-integration and common trends analysis with score-driven models: an application to the Federal Funds effective rate and the US inflation rate. Working Paper 19-08, University Carlos III of Madrid, Department of Economics, 2019. https://e-archivo.uc3m.es/bitstream/handle/10016/28451/we1908.pdf

Blazsek, S., Hernández, H., 2018. Analysis of electricity prices for Central American countries using dynamic conditional score models. Empirical Economics 55 (4): 1807–1848. doi: 10.1007/s00181-017-1341-3.

Blazsek, S., Ho, H.-C., 2017. Markov regime-switching Beta-t-EGARCH. Applied Economics 49 (47): 4793–4805. doi: 10.1080/00036846.2017.1293794.

Blazsek, S., Ho, H.-C., Liu, S.-P., 2018. Score-driven Markov-switching EGARCH models: an application to systematic risk analysis. Applied Economics 50 (56): 6047–6060. doi: 10.1080/00036846.2018.1488073.

Blundell, R., Griffith, R., Windmeijer, F., 2002. Individual effects and dynamic in count data models. Journal of Econometrics 108 (1): 113–131. doi: 10.1016/S0304-4076(01)00108-7.

Bollerslev, T., 1986. Generalized autoregressive conditional heteroskedasticity. Journal of Econometrics 31 (3): 307–327. doi: 10.1016/0304-4076(86)90063-1.

Box, G.E.P., Jenkins, G.M., 1970. Time Series Analysis, Forecasting and Control. Holden-Day, San Francisco.

Caivano, M., Harvey, A.C., Luati, A., 2016. Robust time series models with trend and seasonal components. SERIEs Journal of the Spanish Economic Association 7 (1): 99–120. doi: 10.1007/s13209-015-0134-1.

Chen, Q., Filardo, A., He, D., Zhu, F., 2016. Financial crisis, US unconventional monetary policy and international spillovers. Journal of International Money and Finance 67: 62–81. doi: 10.1016/j.jimonfin.2015.06.011.

Cox, D.R., 1981. Statistical analysis of time series: some recent developments. Scandinavian Journal of Statistics 8 (2): 93–115. https://www.jstor.org/stable/4615819.

Creal, D., Koopman, S.J., Lucas, A., 2011. A dynamic multivariate heavy-tailed model for time-varying volatilities and correlations. Journal of Business & Economic Statistics 29 (4): 552–563. doi: 10.1198/jbes.2011.10070.

Creal, D., Koopman, S.J., Lucas, A., 2013. Generalized autoregressive score models with applications. Journal of Applied Econometrics 28 (5): 777–795. doi: 10.1002/jae.1279.

Cukierman, A., 2013. Monetary policy and institutions before, during, and after the global financial crisis. Journal of Financial Stability 9 (3): 373–384. doi: 10.1016/j.jfs.2013.02.002.

Dickey, D.A., Fuller, W.A., 1979. Distribution of the estimators for autoregressive time series with a unit root. Journal of the American Statistical Association 74 (36): 427–431. doi: 10.2307/2286348.

Elder, J., Serletis, A., 2010. Oil price uncertainty. Journal of Money, Credit and Banking 42 (6): 1137–1159. doi: 10.1111/j.1538-4616.2010.00323.x.

Engle, R.F., 1982. Autoregressive conditional heteroscedasticity with estimates of the variance of United Kingdom inflation. Econometrica 50 (4): 987–1007. doi: 10.2307/1912773.

Escanciano, J.C., Lobato, I.N., 2009. An automatic Portmanteau test for serial correlation. Journal of Econometrics 151 (2): 140–149. doi: 10.1016/j.jeconom.2009.03.001.

Francis, N.R., Jackson, L.E., Owyang, M.T., 2019. How has empirical monetary policy analysis in the U.S. changed after the financial crisis? Economic Modelling. doi: 10.1016/j.econmod.2019.04.022.

Friedman, M., 1977. Nobel lecture: inflation and unemployment. Journal of Political Economy 85 (3): 451–472. doi: 10.1086/260579.

Gouriéroux, C., Monfort, A., Trognon, A., 1984. Pseudo maximum likelihood methods: theory. Econometrica 52 (3): 681–700. doi: 10.2307/1913471.

Guo, H., Klisen, K.L., 2005. Oil price volatility and U.S. macroeconomic activity. Federal Reserve Bank of St. Louis Review, 87 (6): 669–684. doi: 10.20955/r.87.669-84.

Hamilton, J.D., 1989. A new approach to the economic analysis of nonstationary time series and the business cycle. Econometrica 57 (2): 357–384. doi: 10.2307/1912559.

Hamilton, J.D., 1994. Time Series Analysis. Princeton University Press, Princeton.

Hamilton, J.D., 2003. What is an oil shock? Journal of Econometrics 113 (2): 363–398. doi: 10.1016/S0304-4076(02)00207-5.

Hamilton, J.D., Herrera, A.M., 2004. Oil shocks and aggregate macroeconomic behavior: the role of monetary policy: comment. Journal of Money, Credit and Banking 36 (2): 265–286. doi: 10.1353/mcb.2004.0012.

Harvey, A.C., 1989. Forecasting, Structural Time Series Models and the Kalman Filter. Cambridge University Press, Cambridge.

Harvey, A.C., 2013. Dynamic Models for Volatility and Heavy Tails. Cambridge University Press, Cambridge.

Harvey, A.C., Chakravarty, T., 2008. Beta-t-(E)GARCH. Cambridge Working Papers in Economics 0840, Faculty of Economics, University of Cambridge. http://www.econ.cam.ac.uk/research-files/repec/cam/pdf/cwpe0840.pdf.

Harvey, A.C., Luati, A., 2014. Filtering with heavy tails. Journal of the American Statistical Association 109 (507): 1112–1122. doi: 10.1080/01621459.2014.887011.

Hindrayanto, I., Jacobs, J.P.A.M., Osborn, D.R., Tian, J., 2018. Trend-cycle-seasonal interactions: identification and estimation. Macroeconomic Dynamics, 1–26. doi: 10.1017/S1365100517001092.

Hubrich, K., Teräsvirta, T., 2013. Thresholds and smooth transitions in vector autoregressive models (pp. 273–326). In: T.B. Fomby, L. Kilian, and A. Murphy, eds., VAR Models in Macroeconomics – New Developments and Applications: Essays in Honor of Christopher A. Sims (Advances in Econometrics, Vol. 32). Emerald Group Publishing, Cambridge.

Kalman, R.E., 1960. A new approach to linear filtering and prediction problems. Journal of Basic Engineering 82 (D): 35–45. doi: 10.1115/1.3662552.

Kilian, L., 2008a. The economic effects of energy price shocks. Journal of Economic Literature 46 (4): 871–909. doi: 10.1257/jel.46.4.871.

Kilian, L., 2008b. A comparison of the effects of exogenous oil supply shocks on output and inflation in the G7 countries. Journal of the European Economic Association 6 (1): 78–121. doi: 10.1162/JEEA.2008.6.1.78.

Kilian, L., 2009. Not all oil price shocks are alike: disentangling demand and supply shocks in the crude oil market. American Economic Review 99 (3): 1053–1069. doi: 10.1257/aer.99.3.1053.

Kilian, L., 2010. Oil price volatility: origins and effects. Background paper prepared for the World Trade Report 2010, Trade in Natural Resources: Challenges in Global Governance, World Trade Organization. https://www.wto.org/english/res_e/publications_e/wtr10_forum_e/wtr10_kilian_e.htm.

Kilian, L., Lewis, L.T., 2011. Does the FED respond to oil price shocks? The Economic Journal 121 (555): 1047–1072. doi: 10.1111/j.1468-0297.2011.02437.x.

Kilian, L., Lütkepohl, H., 2017. Structural Vector Autoregressive Analysis. Cambridge University Press, Cambridge.

Kim, C.J., Nelson, C.R., 1999. State-Space Models with Regime Switching. The MIT Press, Cambridge.

Klaassen, F., 2002. Improving GARCH volatility forecasts with regime-switching GARCH. Empirical Economics 27 (2): 363–394. doi: 10.1007/s001810100100.

Krolzig, H.-M., 1997. Markov-Switching Vector Autoregressions: Modelling, Statistical Inference, and Application to Business Cycle Analysis. Springer Verlag, Berlin.

Lütkepohl, H., 2005. New Introduction to Multivariate Time Series Analysis. Springer Verlag, Berlin.

Newey, K., West, K.D., 1987. A simple, positive semi-definite, heteroskedasticity and autocorrelation consistent covariance matrix. Econometrica 55 (3): 703–708. doi: 10.2307/1913610.

Nordhaus, W.D., Houthakker, H.S., Sachs, J.D., 1980. Oil and economic performance in industrial countries. Brookings Papers on Economic Activity 2: 341–399. doi: 10.2307/2534326.

Peersman, G., Van Robays, I., 2009. Oil and the Euro Area Economy. Economic Policy 24 (60): 603–651. doi: 10.1111/j.1468-0327.2009.00233.x.

Pestana Barros, C., Gil-Alana, L.A., Payne, J.E., 2011. An analysis of oil production by OPEC countries: persistence, breaks, and outliers. Energy Policy 39 (1): 442–453. doi: 10.1016/j.enpol.2010.10.024.

Raunglerdpanyagul, W., 1985. The seasonal pattern of shipping freight rates. Theses and Major Papers, Paper 298, University of Rhode Island.

Romer, C.D., Romer, D.H., Goldfeld, S.M., Friedman, B.M., 1990. New evidence on the monetary transmission mechanism. Brookings Papers on Economic Activity 1: 149–213. doi: 10.2307/2534527.

Wooldridge, J.M., 2005. Simple solutions to the initial conditions problem in dynamic, nonlinear panel data models with unobserved heterogeneity. Journal of Applied Econometrics 20 (1): 39–54. doi: 10.1002/jae.770.

Ye, M., Zyren, J., Shore, J., 2006. Forecasting short-run crude oil price using high- and low-inventory variables. Energy Policy 34 (17): 2736–2743. doi: 10.1016/j.enpol.2005.03.017.

Appendix A

Each element of the seasonality component is modeled as:

$$s_{k,t} = D_t' \rho_{k,t} = D_{1,t}\rho_{k,1,t} + D_{2,t}\rho_{k,2,t} + \ldots + D_{S,t}\rho_{k,S,t} \tag{A.1}$$

The vector of dynamic seasonal parameters is $\rho_{k,1}$ for $t = 1$ and $\rho_{k,t} = \rho_{k,t-1} + \gamma_{k,t}u_{k,t-1}$ for $t = 2, \ldots, T$. By recursive substitution, the following representation is obtained: $\rho_{k,t} = \rho_{k,1} + \gamma_{k,2}u_{k,1} + \ldots + \gamma_{k,t}u_{k,t-1}$, where $\rho_{k,1}$ is the vector of initial values of $\rho_{k,t}$. Then, each element of $\rho_{k,t}$ is given by

$$\rho_{k,j,t} = \rho_{k,j,1} + \gamma_{k,j,2}u_{k,1} + \ldots + \gamma_{k,j,t}u_{k,t-1} \tag{A.2}$$

for $j = 1, \ldots, S$. By substituting Equation (A.2) into Equation (A.1):

$$\begin{aligned} s_{k,t} &= D_{1,t}(\rho_{k,1,1} + \gamma_{k,1,2}u_{k,1} + \ldots + \gamma_{k,1,t}u_{k,t-1}) \\ &+ D_{2,t}(\rho_{k,2,1} + \gamma_{k,2,2}u_{k,1} + \ldots + \gamma_{k,2,t}u_{k,t-1}) \\ &+ D_{3,t}(\rho_{k,3,1} + \gamma_{k,3,2}u_{k,1} + \ldots + \gamma_{k,3,t}u_{k,t-1}) \\ &+ \vdots \\ &+ D_{S,t}(\rho_{k,S,1} + \gamma_{k,S,2}u_{k,1} + \ldots + \gamma_{k,S,t}u_{k,t-1}) \end{aligned} \tag{A.3}$$

In Equation (A.3), the dummy variables select each one of the terms consecutively for each t. The selected value of $s_{k,t}$ is zero on average for consecutive $j = 1, \ldots, S$ time periods, because the average of each term within the parentheses of Equation (A.3) is zero. To see this, consider first the NLS procedure used for the estimation of the initial values of $\rho_{k,t}$, which ensures that $\rho_{k,1,1} + \rho_{k,2,1} + \ldots + \rho_{k,S,1} = 0$. Thus, $(\rho_{k,1,1} + \rho_{k,2,1} + \ldots + \rho_{k,S,1})/S = 0$. For all terms where $\gamma_{k,j,t}$ appears, $\gamma_{k,1,t} + \gamma_{k,2,t} + \ldots + \gamma_{k,S,t} = 0$, because for $j = 1, \ldots, S$, $\gamma_{k,j,t} = \gamma_{k,j}$ for $D_{j,t} = 1$ and $\gamma_{k,j,t} = -\gamma_{k,j}/(S-1)$ for $D_{j,t} = 0$. Thus, $(\gamma_{k,1,t}u_{k,t-1} + \gamma_{k,2,t}u_{k,t-1} + \ldots + \gamma_{k,S,t}u_{k,t-1})/S = 0$, and the average of $s_{k,t}$ is also zero.

Appendix B

For MS-Seasonal-QVAR, the conditional distribution of y_t depends on r_t, due to the fact that past values of r_t are integrated out in the expectations that define $\mu_{t-1}(r_t)$, $\rho_{k,t-1}(r_t)$ and $u_{t-1}(r_t)$. In this appendix, the computation of those expectations is presented:

$$\begin{aligned}\mu_{t-1}(r_t=1) &= E[\mu_{t-1}(r_{t-1})|y_1,\ldots,y_{t-1},r_t=1] \\ &= \mu_{t-1}(r_{t-1}=1)\Pr(r_{t-1}=1|y_1,\ldots,y_{t-1},r_t=1)+ \\ &\quad \mu_{t-1}(r_{t-1}=2)\Pr(r_{t-1}=2|y_1,\ldots,y_{t-1},r_t=1)\end{aligned} \tag{B.1}$$

$$\begin{aligned}\mu_{t-1}(r_t=2) &= E[\mu_{t-1}(r_{t-1})|y_1,\ldots,y_{t-1},r_t=2] \\ &= \mu_{t-1}(r_{t-1}=1)\Pr(r_{t-1}=1|y_1,\ldots,y_{t-1},r_t=2)+ \\ &\quad \mu_{t-1}(r_{t-1}=2)\Pr(r_{t-1}=2|y_1,\ldots,y_{t-1},r_t=2)\end{aligned} \tag{B.2}$$

$$\begin{aligned}\rho_{k,t-1}(r_t=1) &= E[\rho_{k,t-1}(r_{t-1})|y_1,\ldots,y_{t-1},r_t=1] \\ &= \rho_{k,t-1}(r_{t-1}=1)\Pr(r_{t-1}=1|y_1,\ldots,y_{t-1},r_t=1)+ \\ &\quad \rho_{k,t-1}(r_{t-1}=2)\Pr(r_{t-1}=2|y_1,\ldots,y_{t-1},r_t=1)\end{aligned} \tag{B.3}$$

$$\begin{aligned}\rho_{k,t-1}(r_t=2) &= E[\rho_{k,t-1}(r_{t-1})|y_1,\ldots,y_{t-1},r_t=2] \\ &= \rho_{k,t-1}(r_{t-1}=1)\Pr(r_{t-1}=1|y_1,\ldots,y_{t-1},r_t=2)+ \\ &\quad \rho_{k,t-1}(r_{t-1}=2)\Pr(r_{t-1}=2|y_1,\ldots,y_{t-1},r_t=2)\end{aligned} \tag{B.4}$$

$$\begin{aligned}u_{t-1}(r_t=1) &= E[u_{t-1}(r_{t-1})|y_1,\ldots,y_{t-1},r_t=1] \\ &= u_{t-1}(r_{t-1}=1)\Pr(r_{t-1}=1|y_1,\ldots,y_{t-1},r_t=1)+ \\ &\quad u_{t-1}(r_{t-1}=2)\Pr(r_{t-1}=2|y_1,\ldots,y_{t-1},r_t=1)\end{aligned} \tag{B.5}$$

$$
\begin{aligned}
u_{t-1}(r_t = 2) &= E[u_{t-1}(r_{t-1})|y_1, \ldots, y_{t-1}, r_t = 2] \\
&= u_{t-1}(r_{t-1} = 1) \Pr(r_{t-1} = 1|y_1, \ldots, y_{t-1}, r_t = 2) + \\
&\quad u_{t-1}(r_{t-1} = 2) \Pr(r_{t-1} = 2|y_1, \ldots, y_{t-1}, r_t = 2)
\end{aligned} \tag{B.6}
$$

The probabilities of Equations (B.1) to (B.6) are given by

$$
\Pr(r_{t-1} = 1|y_1, \ldots, y_{t-1}, r_t = 1) = \frac{p\tilde{\pi}_{t-1}(1)}{p\tilde{\pi}_{t-1}(1) + (1-q)\tilde{\pi}_{t-1}(2)} \tag{B.7}
$$

$$
\Pr(r_{t-1} = 2|y_1, \ldots, y_{t-1}, r_t = 1) = 1 - \Pr(r_{t-1} = 1|y_1, \ldots, y_{t-1}, r_t = 1) \tag{B.8}
$$

$$
\Pr(r_{t-1} = 1|y_1, \ldots, y_{t-1}, r_t = 2) = \frac{(1-p)\tilde{\pi}_{t-1}(1)}{(1-p)\tilde{\pi}_{t-1}(1) + q\tilde{\pi}_{t-1}(2)} \tag{B.9}
$$

$$
\Pr(r_{t-1} = 2|y_1, \ldots, y_{t-1}, r_t = 2) = 1 - \Pr(r_{t-1} = 1|y_1, \ldots, y_{t-1}, r_t = 2) \tag{B.10}
$$

and for the first period $\tilde{\pi}_0(1) = \pi^*(1)$ and $\tilde{\pi}_0(2) = \pi^*(2)$ are used, as initial probabilities.

Table 1. Descriptive statistics.

Panel A. Descriptive statistics	World crude oil production growth y_{1t}	US industrial production growth y_{2t}
Start date	February 1973	February 1973
End date	April 2019	April 2019
Sample size T	555	555
Minimum	−9.9073	−4.4337
Maximum	6.4986	2.0506
Mean	0.0732	0.1585
Standard deviation	1.5224	0.7153
Skewness	−1.6452	−1.3149
Excess kurtosis	10.4297	6.1412
ADF	-25.5561^{***}	-8.3432^{***}
Panel B. Seasonality effects	**World crude oil production growth y_{1t}**	**US industrial production growth y_{2t}**
δ_{Jan}	$-0.9737^{***}(0.3301)$	$-0.0448(0.1244)$
δ_{Feb}	$0.2798(0.2327)$	$0.2180^{*}(0.1133)$
δ_{Mar}	$0.0117(0.1485)$	$0.1559^{*}(0.0915)$
δ_{Apr}	$-0.2615^{*}(0.1536)$	$0.1370(0.1008)$
δ_{May}	$-0.1636(0.1731)$	$0.1662^{*}(0.0950)$
δ_{Jun}	$0.1767(0.1951)$	$0.1577^{**}(0.0672)$
δ_{Jul}	$0.7302^{***}(0.1966)$	$0.1652^{**}(0.0758)$
δ_{Aug}	$-0.2276(0.2050)$	$0.2212^{**}(0.0946)$
δ_{Sep}	$0.4115^{*}(0.2467)$	$0.1157(0.1303)$
δ_{Oct}	$0.4208^{+}(0.2876)$	$0.2816^{***}(0.0900)$
δ_{Nov}	$0.4005^{**}(0.1651)$	$0.1798^{+}(0.1157)$
δ_{Dec}	$0.0780(0.1627)$	$0.1479(0.1326)$

Notes: Growth in variables is measured in percentage points. HAC standard errors are reported in parentheses. $^{+}$, *, ** and *** indicate significance at the 15%, 10%, 5% and 1% levels, respectively.

Table 2. Parameter estimates and model diagnostics for Seasonal-QVAR and classical alternatives.

Seasonal-QVAR				Basic structural model		Gaussian Seasonal-VARMA			
c_1	0.1416***(0.0474)	$\gamma_{2,\text{Jan}}$	−0.1319(0.0995)	c_1	0.1010(0.2434)	c_1	0.0693**(0.0338)	$\gamma_{2,\text{Jan}}$	0.0089(0.0280)
c_2	0.1274***(0.0487)	$\gamma_{2,\text{Feb}}$	−0.1562**(0.0714)	c_2	0.2073(0.2657)	c_2	0.1689***(0.0387)	$\gamma_{2,\text{Feb}}$	−0.1500***(0.0478)
$\Phi_{1,1}$	0.5257***(0.1891)	$\gamma_{2,\text{Mar}}$	0.0416*(0.0225)	$\Phi_{1,1}$	−0.2038*(0.1107)	$\Phi_{1,1}$	0.5856***(0.0703)	$\gamma_{2,\text{Mar}}$	0.1994*(0.1033)
$\Phi_{1,2}$	0.1211(0.0871)	$\gamma_{2,\text{Apr}}$	0.2319***(0.0737)	$\Phi_{1,2}$	0.3053^{+}(0.1914)	$\Phi_{1,2}$	0.2357***(0.0730)	$\gamma_{2,\text{Apr}}$	−0.0536(0.0844)
$\Phi_{2,1}$	−0.4515(0.3779)	$\gamma_{2,\text{May}}$	−0.5553***(0.2088)	$\Phi_{2,1}$	−0.2607^{+}(0.1766)	$\Phi_{2,1}$	−0.0769*(0.0425)	$\gamma_{2,\text{May}}$	−0.0390(0.0600)
$\Phi_{2,2}$	0.9971***(0.0933)	$\gamma_{2,\text{Jun}}$	0.0019(0.0402)	$\Phi_{2,2}$	0.8948***(0.0870)	$\Phi_{2,2}$	0.8305***(0.0428)	$\gamma_{2,\text{Jun}}$	0.0085(0.0197)
$\Psi_{1,1}$	−0.0869(0.0965)	$\gamma_{2,\text{Jul}}$	−0.1650(0.1538)	$\Omega^{-1}_{v,1,1}$	0.7632*(0.4078)	$\Psi_{1,1}$	−0.2412***(0.0709)	$\gamma_{2,\text{Jul}}$	−0.1032(0.1007)
$\Psi_{1,2}$	−0.0460(0.0883)	$\gamma_{2,\text{Aug}}$	0.0527(0.0499)	$\Omega^{-1}_{v,2,1}$	−0.4145***(0.1147)	$\Psi_{1,2}$	0.0585(0.0507)	$\gamma_{2,\text{Aug}}$	0.0208(0.0400)
$\Psi_{2,1}$	0.0598^{+}(0.0381)	$\gamma_{2,\text{Sep}}$	−0.0696(0.0993)	$\Omega^{-1}_{v,2,2}$	0.0000(0.0005)	$\Psi_{2,1}$	0.0018(0.0162)	$\gamma_{2,\text{Sep}}$	−0.1410***(0.0524)
$\Psi_{2,2}$	0.3746***(0.0773)	$\gamma_{2,\text{Oct}}$	−0.0069(0.0460)	$\Omega^{-1}_{\eta,1,1}$	1.2032***(0.2515)	$\Psi_{2,2}$	0.2827***(0.0304)	$\gamma_{2,\text{Oct}}$	−0.0606(0.0408)
$\Omega^{-1}_{v,1,1}$	0.9242***(0.0325)	$\gamma_{2,\text{Nov}}$	−0.0377(0.0691)	$\Omega^{-1}_{\eta,2,1}$	0.3591**(0.1430)	$\Omega^{-1}_{v,1,1}$	1.4116***(0.0366)	$\gamma_{2,\text{Nov}}$	0.0775(0.0566)
$\Omega^{-1}_{v,2,1}$	0.0552**(0.0244)	$\gamma_{2,\text{Dec}}$	0.0935(0.1150)	$\Omega^{-1}_{\eta,2,2}$	0.2501***(0.0348)	$\Omega^{-1}_{v,2,1}$	0.1013***(0.0263)	$\gamma_{2,\text{Dec}}$	−0.0070(0.0179)
$\Omega^{-1}_{v,2,2}$	0.4549***(0.0155)	C_1	0.7909	$\sigma_{\xi,1}$	0.0331***(0.0094)	$\Omega^{-1}_{v,2,2}$	0.6286***(0.0162)	C_1	0.7103
ν	3.5255***(0.2899)	C_2 to C_4 ADF	All stationary	$\sigma_{\xi,2}$	0.0000(0.0037)	$\gamma_{1,\text{Jan}}$	−0.6723***(0.1499)	MDS $v_{1,t}$	0.6401
$\gamma_{1,\text{Jan}}$	−0.0534(0.1814)	C_3	0.7132	C_1	0.8168	$\gamma_{1,\text{Feb}}$	−0.1083(0.0954)	MDS $v_{2,t}$	0.4874
$\gamma_{1,\text{Feb}}$	0.0728(0.2314)	C_4	0.5146	MDS $v_{1,t}$	0.8817	$\gamma_{1,\text{Mar}}$	0.2775***(0.0976)	LL	−2.7183
$\gamma_{1,\text{Mar}}$	0.5342^{+}(0.3583)	Q_t ADF	All stationary	MDS $v_{2,t}$	0.8909	$\gamma_{1,\text{Apr}}$	0.3476***(0.1285)	AIC	5.5700
$\gamma_{1,\text{Apr}}$	0.0833(0.2334)	MDS $v_{1,t}$	0.2116	LL	−2.8375	$\gamma_{1,\text{May}}$	0.2815***(0.1024)	BIC	5.8579
$\gamma_{1,\text{May}}$	0.3969**(0.1546)	MDS $v_{2,t}$	0.0553	AIC	5.7254	$\gamma_{1,\text{Jun}}$	0.4714***(0.1204)	HQC	5.6825
$\gamma_{1,\text{Jun}}$	0.5691***(0.1870)	MDS $u_{1,t}$	0.2277	BIC	5.8343	$\gamma_{1,\text{Jul}}$	−0.1628(0.1221)		
$\gamma_{1,\text{Jul}}$	−0.8191***(0.1334)	MDS $u_{2,t}$	0.1357	HQC	5.7679	$\gamma_{1,\text{Aug}}$	0.3861***(0.1173)		
$\gamma_{1,\text{Aug}}$	0.0701(0.1777)	LL	**−2.5386**			$\gamma_{1,\text{Sep}}$	−0.1182(0.1348)		
$\gamma_{1,\text{Sep}}$	−0.2525^{+}(0.1736)	AIC	**5.2140**			$\gamma_{1,\text{Oct}}$	0.1574(0.1098)		
$\gamma_{1,\text{Oct}}$	0.5815**(0.2527)	BIC	**5.5098**			$\gamma_{1,\text{Nov}}$	0.0292(0.1084)		
$\gamma_{1,\text{Nov}}$	0.3040(0.2152)	HQC	**5.3296**			$\gamma_{1,\text{Dec}}$	−0.1717(0.1323)		
$\gamma_{1,\text{Dec}}$	−0.1211(0.2017)								

Notes: 'MDS' denotes the p-value of the martingale difference sequence test. Bold numbers indicate superior statistical performance. Standard errors are in parentheses. $^{+}$, *, ** and *** indicate significance at the 15%, 10%, 5% and 1% levels, respectively.

Table 3. Parameter estimates for MS-Seasonal-QVAR.

MS-Seasonal-QVAR, specification: $c(r_t)$, $\mu_t(r_t)$, s_t, $v_t(r_t)$				MS-Seasonal-QVAR, specification: $c(r_t)$, μ_t, s_t, $v_t(r_t)$			
p	0.9976***(0.0002)	$\gamma_{1,\text{Jan}}$	0.1895***(0.0340)	p	0.9976***(0.0028)	$\gamma_{1,\text{Jan}}$	−0.0799(0.1696)
q	0.9981***(0.0001)	$\gamma_{1,\text{Feb}}$	0.1211***(0.0437)	q	0.9982***(0.0019)	$\gamma_{1,\text{Feb}}$	0.2034(0.2088)
$c_1(1)$	0.2687***(0.0315)	$\gamma_{1,\text{Mar}}$	0.3029*(0.1549)	$c_1(1)$	0.2519**(0.1073)	$\gamma_{1,\text{Mar}}$	0.3188(0.2282)
$c_2(1)$	0.1403***(0.0246)	$\gamma_{1,\text{Apr}}$	−0.0450(0.0314)	$c_2(1)$	0.1768**(0.0830)	$\gamma_{1,\text{Apr}}$	0.1268(0.2493)
$c_1(2)$	0.1292***(0.0269)	$\gamma_{1,\text{May}}$	0.3354***(0.0598)	$c_1(2)$	0.0940**(0.0384)	$\gamma_{1,\text{May}}$	0.1894(0.2143)
$c_2(2)$	0.2195***(0.0287)	$\gamma_{1,\text{Jun}}$	0.1286**(0.0553)	$c_2(2)$	0.1046*(0.0578)	$\gamma_{1,\text{Jun}}$	0.5371**(0.2220)
$\Phi_{1,1}(1)$	−0.1087**(0.0530)	$\gamma_{1,\text{Jul}}$	−0.8161***(0.0462)	$\Phi_{1,1}$	0.5368***(0.1056)	$\gamma_{1,\text{Jul}}$	−0.4680**(0.2003)
$\Phi_{1,2}(1)$	0.2821***(0.0205)	$\gamma_{1,\text{Aug}}$	−0.0870***(0.0334)	$\Phi_{1,2}$	0.1678**(0.0727)	$\gamma_{1,\text{Aug}}$	0.0529(0.2364)
$\Phi_{2,1}(1)$	−2.8013***(0.0841)	$\gamma_{1,\text{Sep}}$	−0.3947***(0.0289)	$\Phi_{2,1}$	−0.2270*(0.1335)	$\gamma_{1,\text{Sep}}$	−0.2137(0.1819)
$\Phi_{2,2}(1)$	1.6327***(0.0445)	$\gamma_{1,\text{Oct}}$	0.4007***(0.0346)	$\Phi_{2,2}$	0.9192***(0.0550)	$\gamma_{1,\text{Oct}}$	0.6351**(0.2563)
$\Phi_{1,1}(2)$	0.8648***(0.0602)	$\gamma_{1,\text{Nov}}$	−0.0550(0.0403)			$\gamma_{1,\text{Nov}}$	0.2174(0.2402)
$\Phi_{1,2}(2)$	−0.0326**(0.0150)	$\gamma_{1,\text{Dec}}$	−0.0036(0.0494)			$\gamma_{1,\text{Dec}}$	−0.0412(0.1898)
$\Phi_{2,1}(2)$	0.5612***(0.1136)	$\gamma_{2,\text{Jan}}$	−0.8408***(0.0631)			$\gamma_{2,\text{Jan}}$	0.0196(0.0285)
$\Phi_{2,2}(2)$	0.8800***(0.0442)	$\gamma_{2,\text{Feb}}$	0.2514***(0.0600)			$\gamma_{2,\text{Feb}}$	0.0074(0.0280)
$\Psi_{1,1}(1)$	−0.0295**(0.0129)	$\gamma_{2,\text{Mar}}$	−0.0198(0.0170)	$\Psi_{1,1}$	−0.2434*(0.1326)	$\gamma_{2,\text{Mar}}$	0.2043(0.1467)
$\Psi_{1,2}(1)$	0.2543***(0.0345)	$\gamma_{2,\text{Apr}}$	0.1588***(0.0366)	$\Psi_{1,2}$	0.0072(0.0783)	$\gamma_{2,\text{Apr}}$	−0.0710(0.0999)
$\Psi_{2,1}(1)$	0.0206(0.0311)	$\gamma_{2,\text{May}}$	−0.4214***(0.0574)	$\Psi_{2,1}$	−0.0021(0.0301)	$\gamma_{2,\text{May}}$	−0.0786(0.0745)
$\Psi_{2,2}(1)$	0.7459***(0.0876)	$\gamma_{2,\text{Jun}}$	0.0321(0.0348)	$\Psi_{2,2}$	0.3310***(0.0622)	$\gamma_{2,\text{Jun}}$	0.0262(0.0231)
$\Psi_{1,1}(2)$	−0.1000***(0.0366)	$\gamma_{2,\text{Jul}}$	−0.1295***(0.0423)			$\gamma_{2,\text{Jul}}$	−0.2667*(0.1480)
$\Psi_{1,2}(2)$	0.1563***(0.0411)	$\gamma_{2,\text{Aug}}$	0.1624***(0.0342)			$\gamma_{2,\text{Aug}}$	0.0132(0.0302)
$\Psi_{2,1}(2)$	0.0377(0.0315)	$\gamma_{2,\text{Sep}}$	−0.3978***(0.0717)			$\gamma_{2,\text{Sep}}$	−0.0036(0.0456)
$\Psi_{2,2}(2)$	0.1469***(0.0409)	$\gamma_{2,\text{Oct}}$	0.3433***(0.0691)			$\gamma_{2,\text{Oct}}$	0.0506*(0.0267)
$\Omega^{-1}_{v,1,1}(1)$	1.4990***(0.0571)	$\gamma_{2,\text{Nov}}$	−0.0194(0.0176)	$\Omega^{-1}_{v,1,1}(1)$	1.6021***(0.1056)	$\gamma_{2,\text{Nov}}$	−0.0412*(0.0222)
$\Omega^{-1}_{v,2,1}(1)$	0.0999***(0.0277)	$\gamma_{2,\text{Dec}}$	0.2333***(0.0434)	$\Omega^{-1}_{v,2,1}(1)$	0.1208***(0.0375)	$\gamma_{2,\text{Dec}}$	0.1432(0.1068)
$\Omega^{-1}_{v,2,2}(1)$	0.4935***(0.0159)			$\Omega^{-1}_{v,2,2}(1)$	0.5244***(0.0330)		
$\Omega^{-1}_{v,1,1}(2)$	0.6474***(0.0189)			$\Omega^{-1}_{v,1,1}(2)$	0.6494***(0.0310)		
$\Omega^{-1}_{v,2,1}(2)$	0.0338(0.0273)			$\Omega^{-1}_{v,2,1}(2)$	0.0335(0.0278)		
$\Omega^{-1}_{v,2,2}(2)$	0.4396***(0.0154)			$\Omega^{-1}_{v,2,2}(2)$	0.4826***(0.0242)		
$\nu(1)$	3.9071***(0.3172)			$\nu(1)$	4.3035***(0.7450)		
$\nu(2)$	6.8669***(0.6030)			$\nu(2)$	7.9438***(1.8892)		

Notes: Standard errors are in parentheses. *, ** and *** indicate significance at the 10%, 5% and 1% levels, respectively.

Table 4. Model diagnostics for MS-Seasonal-QVAR.

MS-Seasonal-QVAR, specification: $c(r_t)$, $\mu_t(r_t)$, s_t, $v_t(r_t)$		MS-Seasonal-QVAR, specification: $c(r_t)$, μ_t, s_t, $v_t(r_t)$	
$C_1(1)$	0.7828	$C_1(1)$	0.7291
$C_1(2)$	0.8828	$C_1(2)$	0.7291
$Q_t(1)$ ADF	All stationary	$Q_t(1)$ ADF	All stationary
$Q_t(2)$ ADF	All stationary	$Q_t(2)$ ADF	All stationary
C_1	0.8810	C_1	0.7291
C_2 to C_4 ADF	All stationary	C_2 to C_4 ADF	All stationary
C_3	0.8773	C_3	0.7321
C_4	0.7771	C_4	0.5443
MDS $E(v_{1,t})$	0.2750	MDS $E(v_{1,t})$	0.4067
MDS $E(v_{2,t})$	0.5628	MDS $E(v_{2,t})$	0.1802
MDS $E(u_{1,t})$	0.4915	MDS $E(u_{1,t})$	0.3310
MDS $E(u_{2,t})$	0.2410	MDS $E(u_{2,t})$	0.3062
LL	**−2.3719**	LL	−2.4098
AIC	**4.9384**	AIC	4.9853
BIC	5.3586	BIC	**5.3433**
HQC	**5.1025**	HQC	5.1252
LR	**42.0726*****		

Notes: 'MDS' denotes the p-value of the martingale difference sequence test. Bold numbers indicate superior statistical performance. Standard errors are in parentheses. The likelihood-ratio (LR) test with $\chi^2(54-46) = \chi^2(8)$ is used in order to compare the LLs of the more general and the more specific models. *** indicates significance at the 1% level.

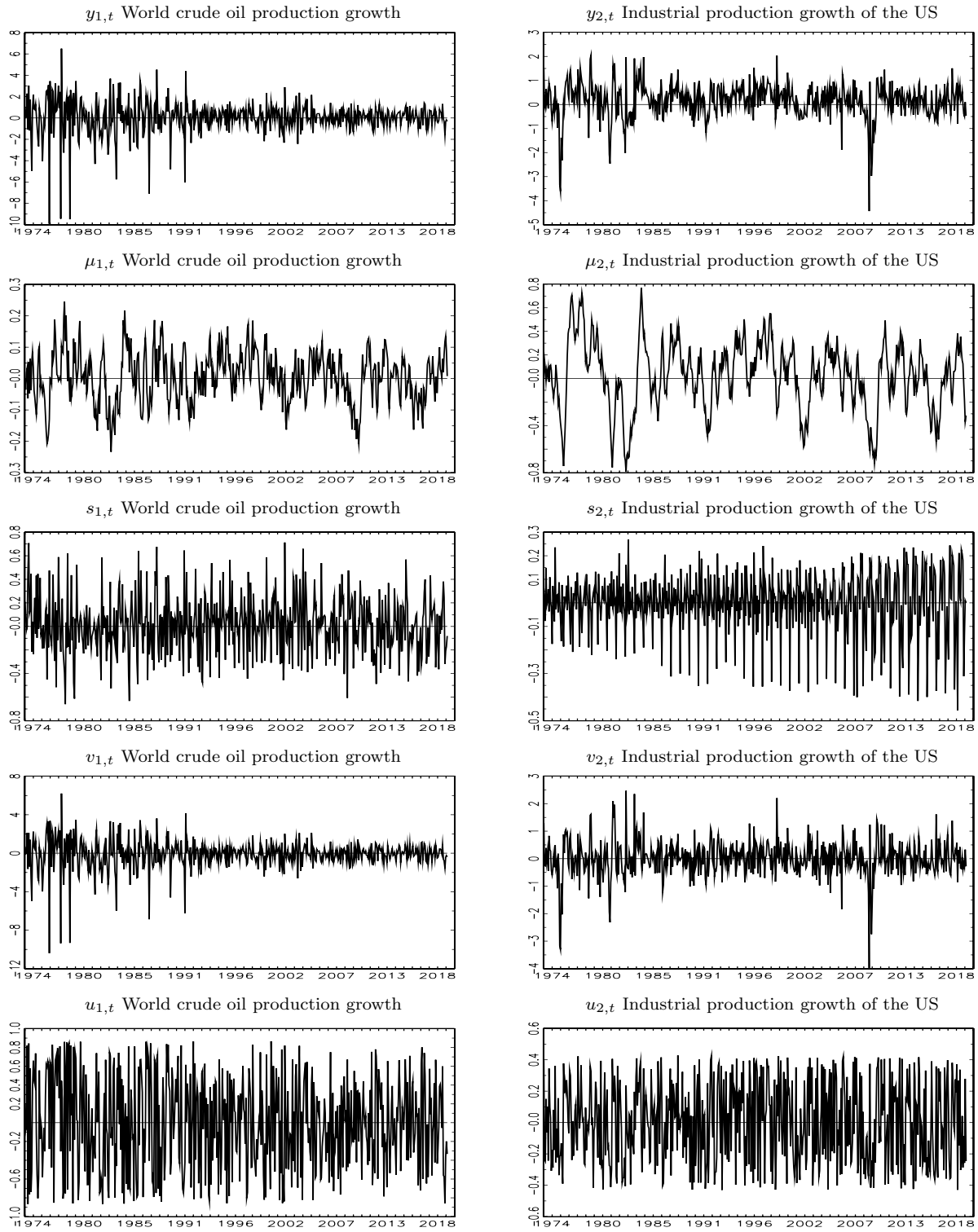

Fig. 1. Time series components for Seasonal-QVAR (March 1973 to April 2019).

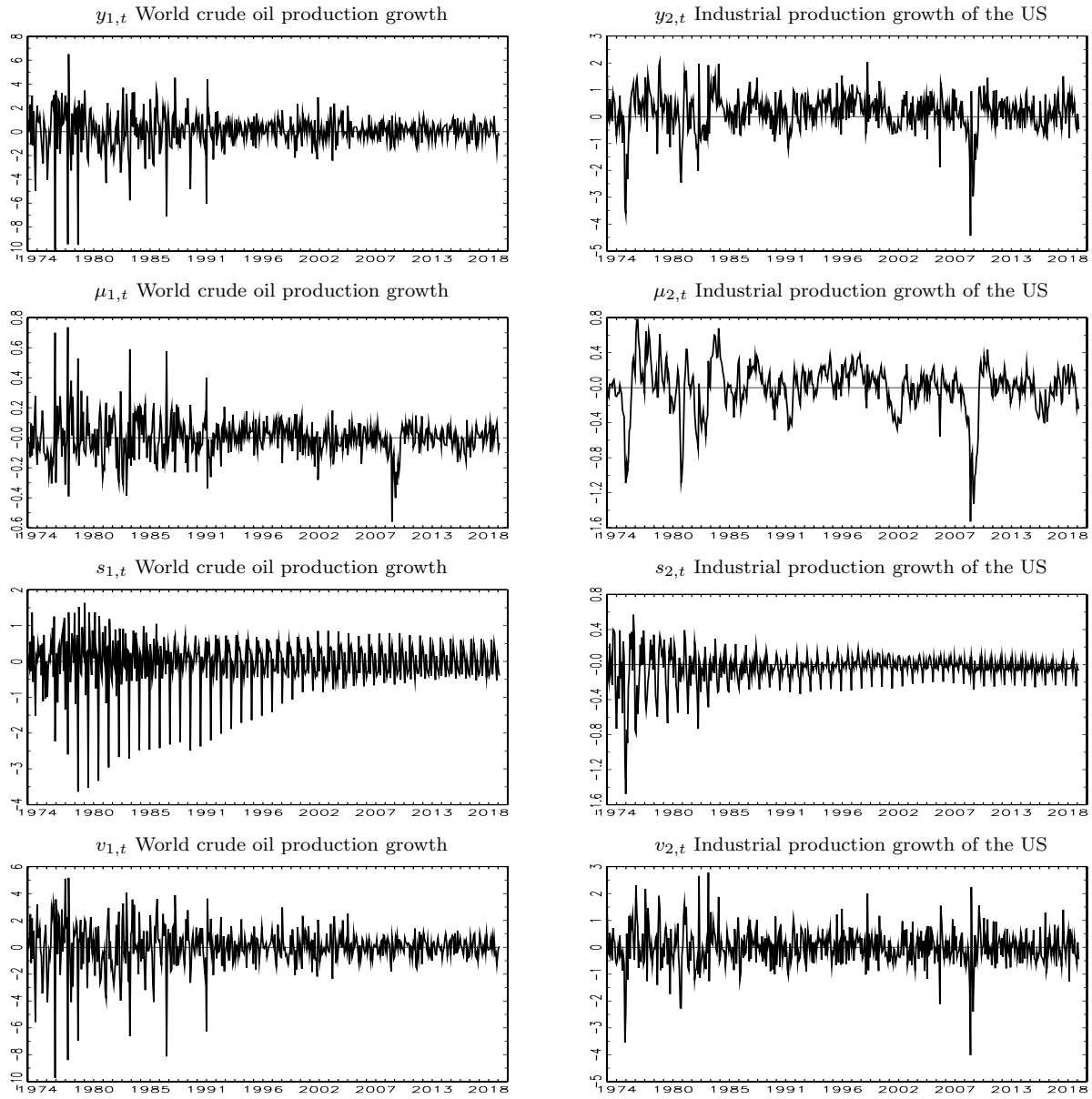

Fig. 2. Time series components for the Basic structural model (March 1973 to April 2019).

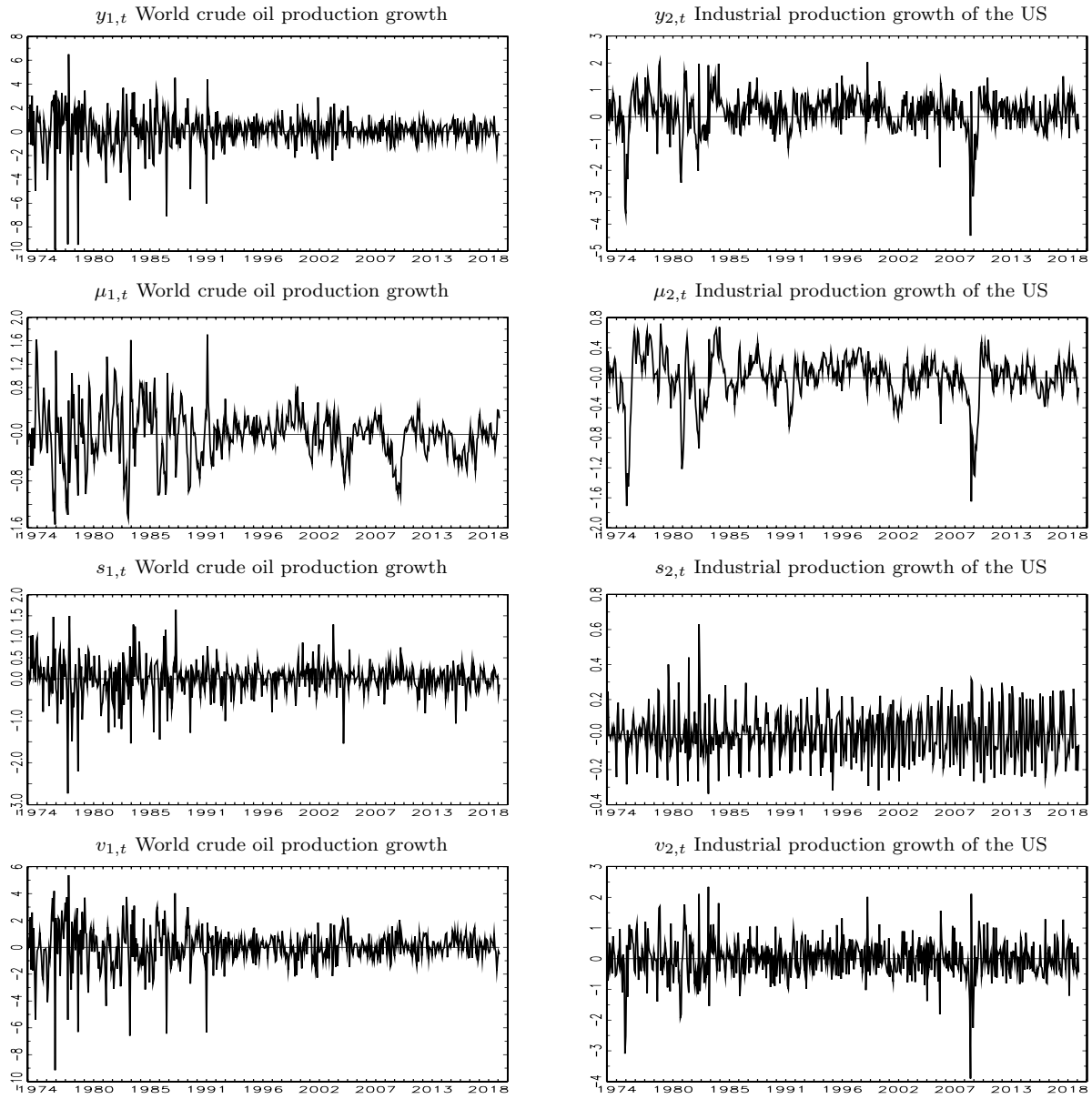

Fig. 3. Time series components for Seasonal-VARMA (March 1973 to April 2019).

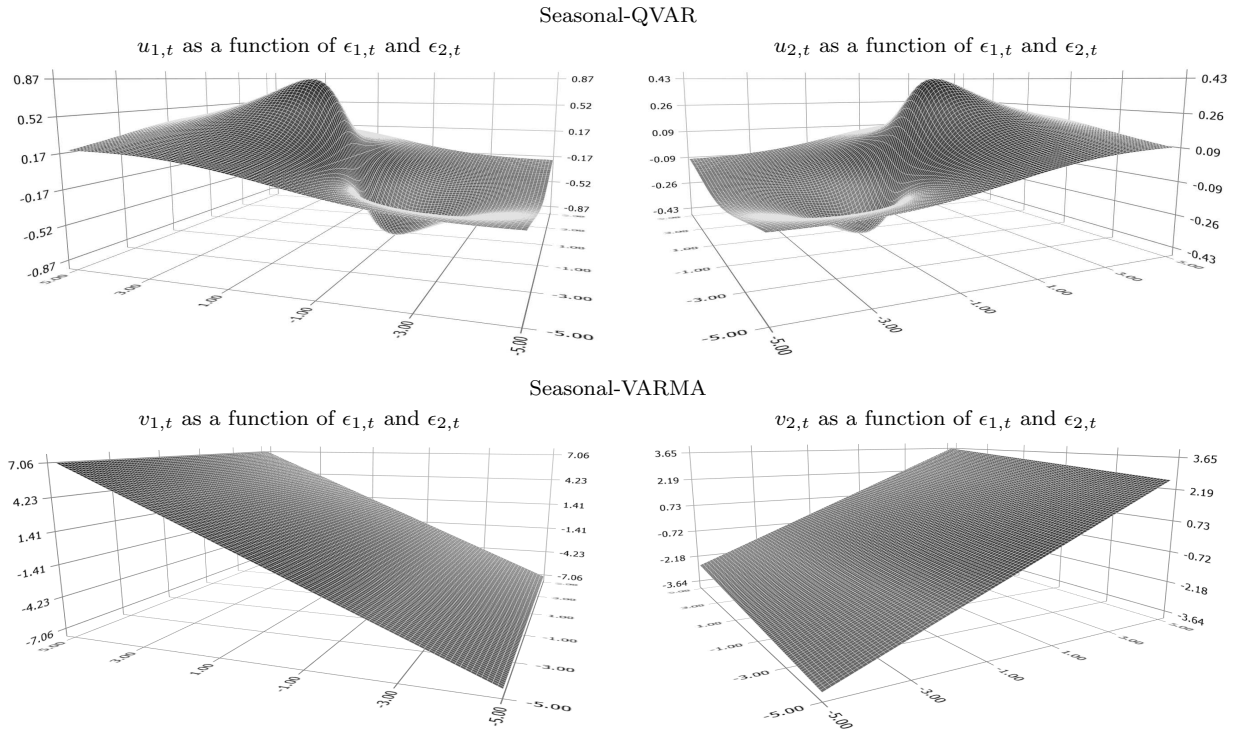

Fig. 4. Robustness of updating terms to extreme values.

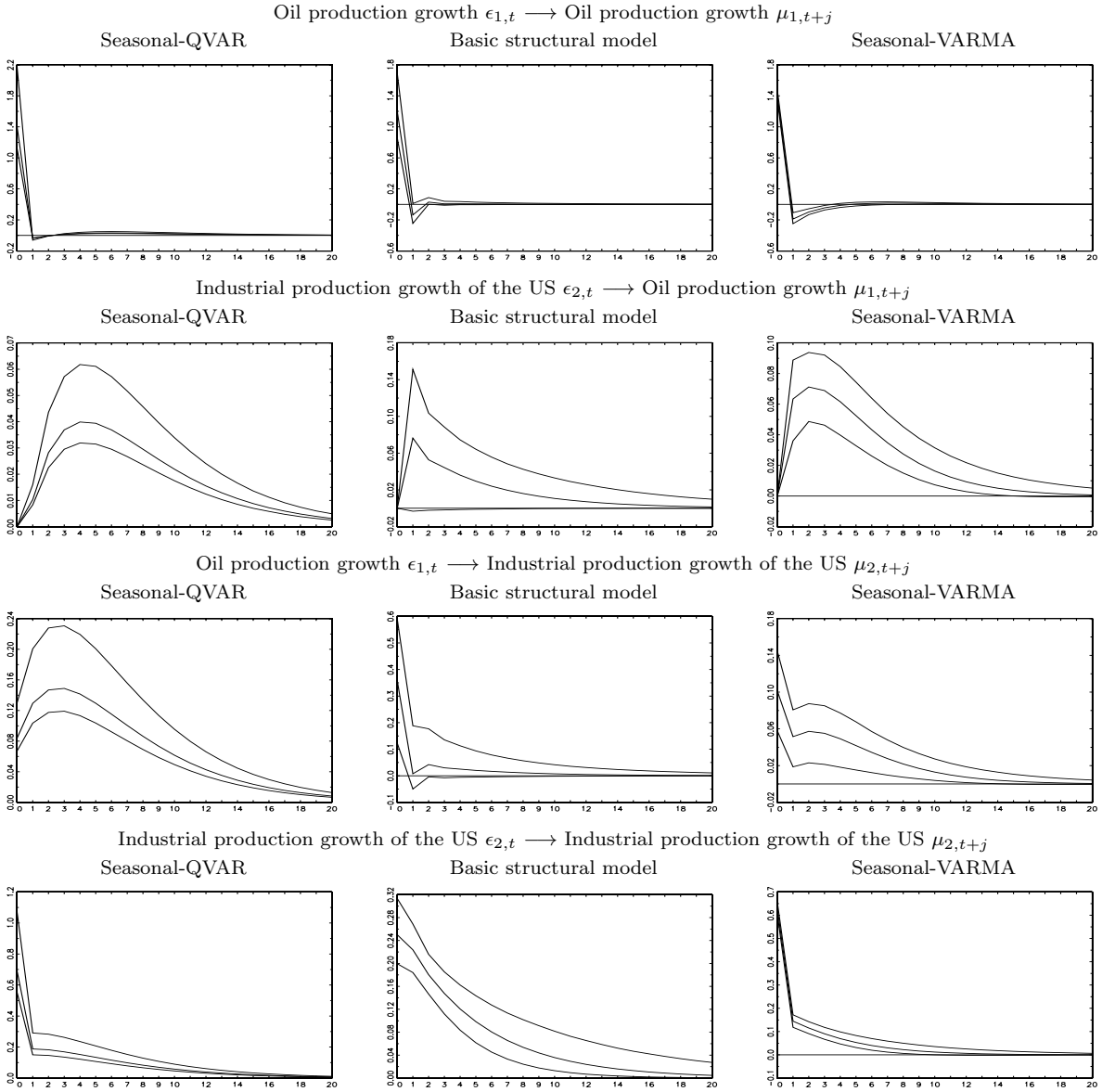

Fig. 5. Impulse response function with 90% confidence interval for Seasonal-QVAR and classical alternatives.

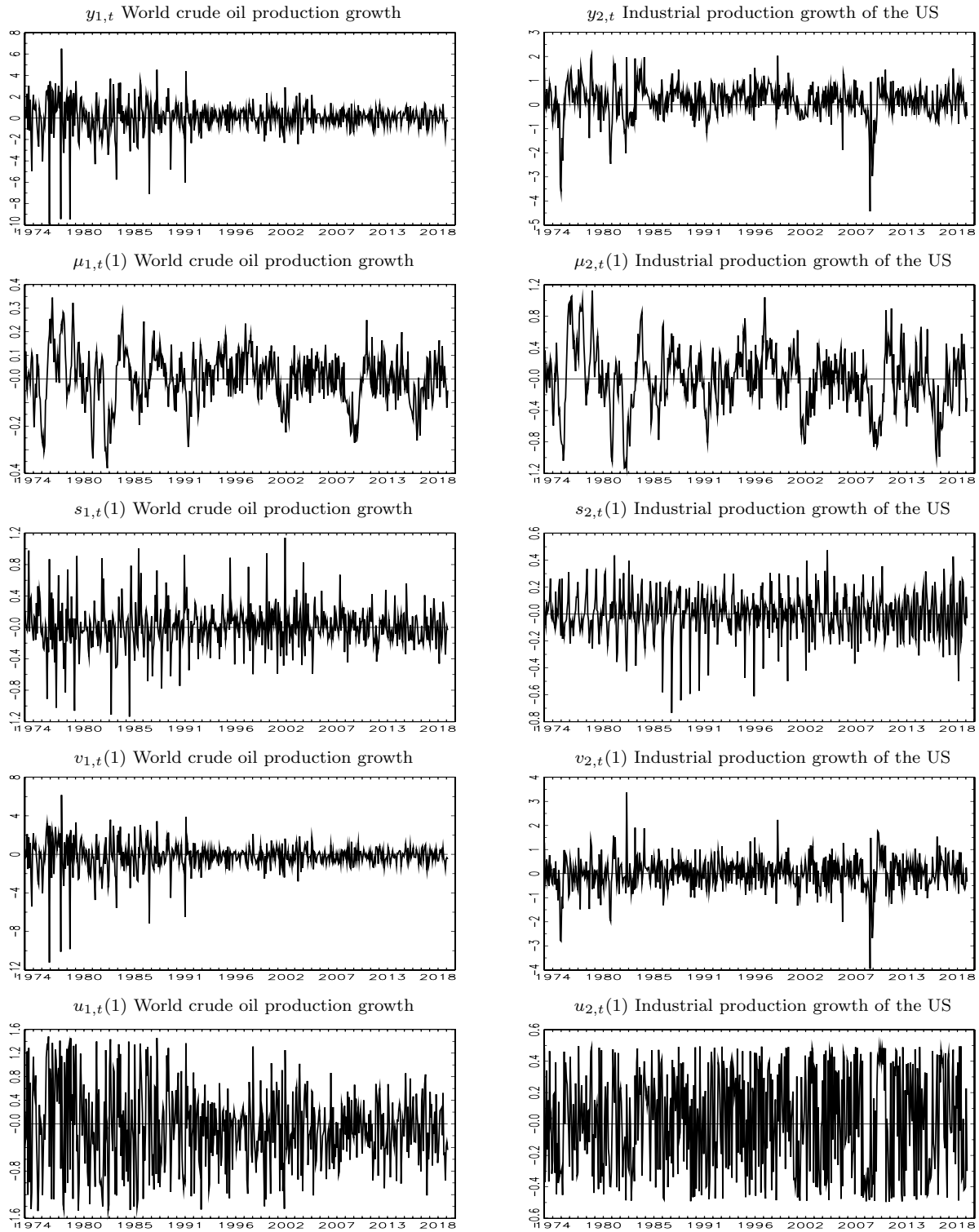

Fig. 6. Time series components of MS-Seasonal-QVAR with $c(r_t)$, $\mu_t(r_t)$, s_t, $v_t(r_t)$ for $r_t = 1$ (March 1973 to April 2019).

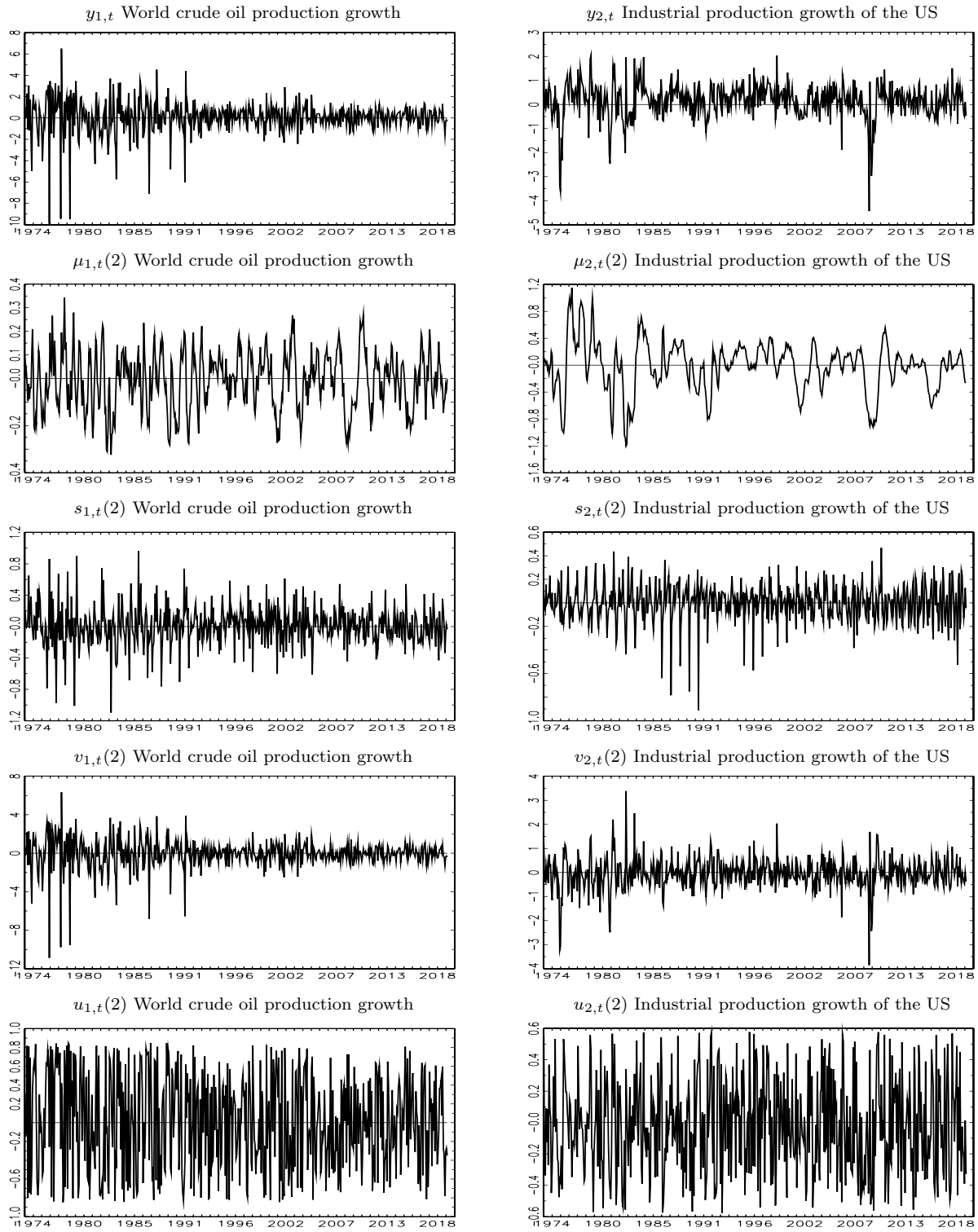

Fig. 7. Time series components of MS-Seasonal-QVAR with $c(r_t)$, $\mu_t(r_t)$, s_t, $v_t(r_t)$ for $r_t = 2$ (March 1973 to April 2019).

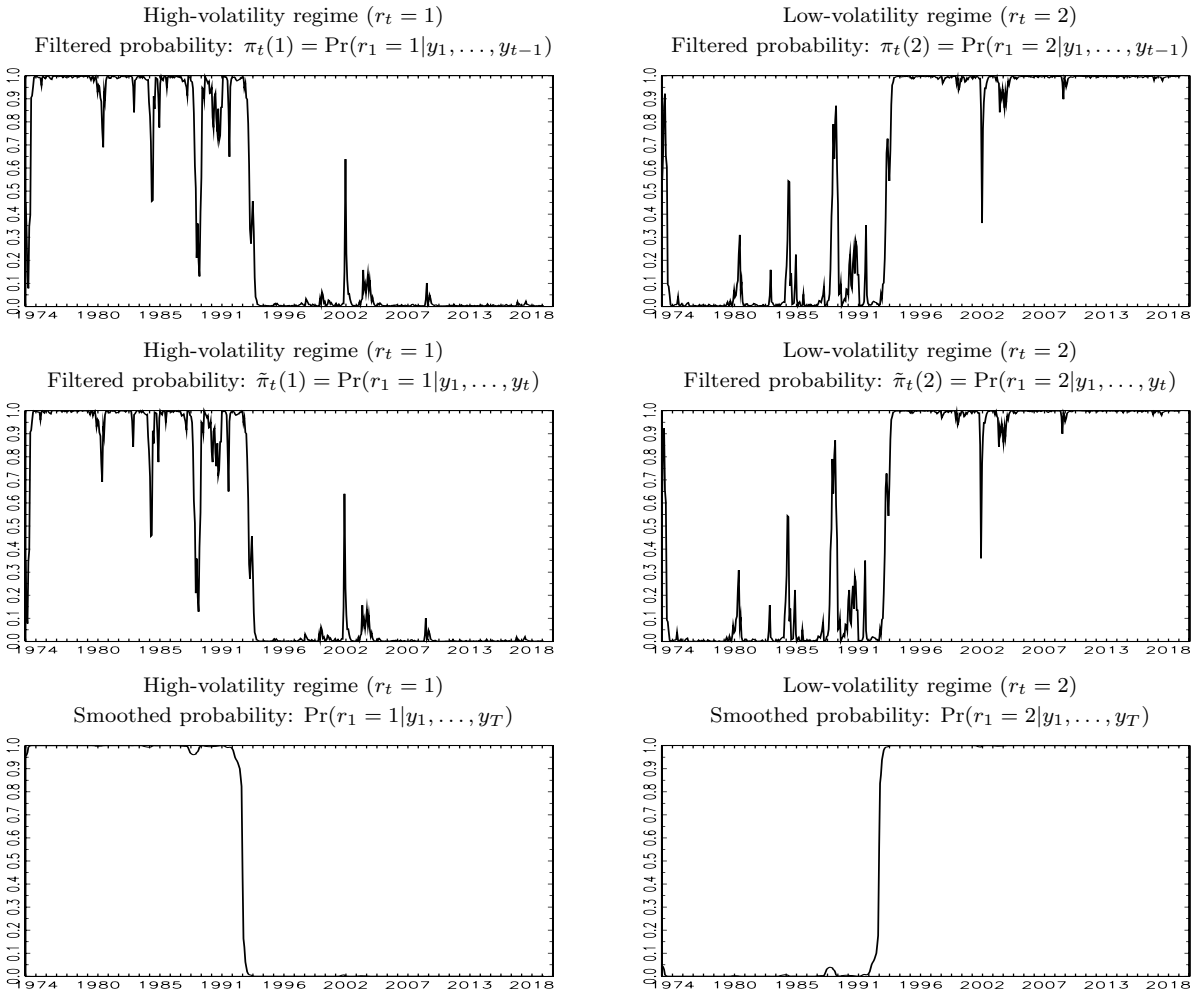

Fig. 8. Filtered and smoothed probabilities for MS-Seasonal-QVAR with $c(r_t)$, $\mu_t(r_t)$, s_t, $v_t(r_t)$ (March 1973 to April 2019).

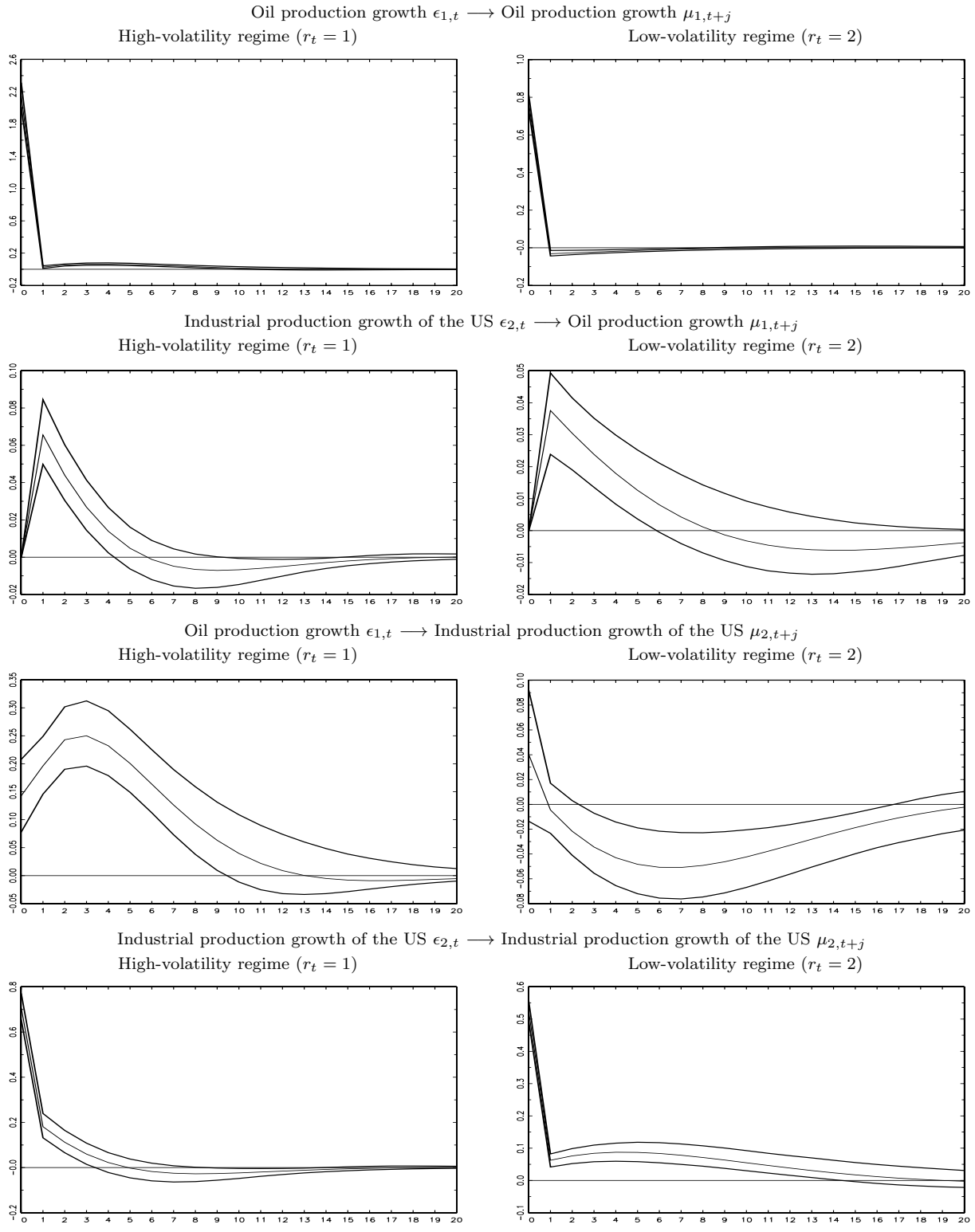

Fig. 9. Impulse response function with 90% confidence interval for MS-Seasonal-QVAR with $c(r_t)$, $\mu_t(r_t)$, s_t, $v_t(r_t)$.